Isotopic constraints on ore-grade enrichment of rare earth elements in carbonatites: the Elk Creek carbonatite example

Philip L. Verplanck[1], G. Lang Farmer[2], Craig A. Johnson[1], Heather A. Lowers[1]
[1]*U.S. Geological Survey, Denver Colorado, USA*
[2]*University of Colorado, Boulder, Colorado USA*

Abstract. Magmatic, hydrothermal, and weathering processes play important roles in enrichment of rare earth elements (REEs) in carbonatites. We utilized multiple isotopic systems to evaluate the origin of the REE mineralization of the Elk Creek carbonatite, Nebraska, United States. Nd and Sr isotopes were used to evaluate the source of the REEs, the age of the carbonatite, and open-system behavior. The ε_{Ndi} (1.9 to 3.0, median of 2.4) is consistent with a lithospheric mantle source for the REEs. Sr_i ranges from 0.70289 to 0.70748. The lower Sr_i values are consistent with a mantle reservoir, but the higher values suggest input from other sources (open-system behavior). Multiple generations of dolomite were observed. Generation 1 (Dol I) is well crystalized, contains inclusions, and is intergrown with coarse apatite. Fine dolomite (Dol II) surrounds Dol I in some units, is poorly crystalline, and contains more Fe, Mn, and Sr than Dol I. Calcium and oxygen isotope analyses of Dol I plot in or near the primary igneous carbonate field, whereas Dol II extends to greater values ($\delta^{13}C$ to -1, $\delta^{18}O$ to 23). Ore-grade REE mineralization occurs in veins that cut units containing Dol II, suggesting that REEs were remobilized and enriched by late-stage fluids.

1 Introduction

Carbonatites are the primary source of niobium and light rare earth elements (REEs) and are potential sources of other critical elements. Compared to many mineral deposit systems, relatively little work has been done to constrain important questions concerning the distribution of mineralized carbonatites, the processes responsible for ore-grade enrichment, and the timing of ore forming processes. Isotope geochemistry can play an important role in addressing these unknowns regarding carbonatite ore genesis because the composition of these intrusive-related deposits lends itself to a multi-isotope approach. Radiogenic isotopes (including Nd, Sr, and Pb) can constrain the age and origin of the ores as well as open versus vs closed system behavior. Stable isotopes (including C, O, and S) can constrain the origin of the ores and open and closed system behavior. It is an ideal situation to have an isotopic system that matches one of the ore commodities, such is the case with neodymium in carbonatites. Strontium is generally quite enriched in carbonatites because of its similar charge and ionic radius to calcium. Similarly, carbonatites lend themselves to calcium and oxygen isotopic analysis because these elements are found in multiple minerals. Sulfide and sulfate minerals are also present in many carbonatites, and thus sulfur isotopes are another tool that can be employed. By utilizing a multi-isotope approach, data can be gathered from a variety of minerals that formed throughout the paragenesis.

This abstract will highlight the utilization of a multi-isotope approach to constrain REE enrichment in the Elk Creek carbonatite, located in southeastern Nebraska, USA. The multi-lithologic Elk Creek carbonatite is associated with other alkaline intrusives. The carbonatite, reported to be the largest niobium resource in the United States, contains zones enriched in REEs. This intrusive complex is buried by more than 200 m of Pennsylvanian marine sedimentary rocks and Quaternary glacial till. Alkaline intrusive units associated with the carbonatite include syenites and subordinate mafic dikes. The carbonatite and alkaline intrusives intrude into Precambrian granite and gneiss on the eastern margin of a major rift zone in the basement rocks (the Mid-Continent rift) where the rift has been offset by one of a series of southeasterly trending structures. Age determinations of the carbonatite range from ~ 500 to 570 Ma.

In 1970, a geophysical survey identified a positive gravity anomaly, and the following year the carbonatite was discovered when drilled by the state of Nebraska (Carlson and Treves 2005). Between 1973 and 1986, Molycorp Inc. undertook an extensive exploration program at the site, including over 100 drill holes that amassed ~46,800 m of core. Our study utilizes a subset of the archived Molycorp drill cores to evaluate REE enrichment in carbonatites. Molycorp geologists divided the carbonatite into three primary lithologies: apatite beforsite, barite beforsite, and magnetite beforsite; beforsite is a dolomite-rich carbonatite. Brecciated carbonatite is also present in some of the cores, and much of the carbonatite was overprinted by various fluids. Zones of ferruginous alteration resemble “rodbergite” as described at the Fen complex, Norway.

2 Geology and geochemistry

The apatite beforsite is the most voluminous carbonatite unit in the Elk Creek complex; it consists of dolomite and apatite with variable amounts of quartz, fluorite, phlogopite, pyroxene, chlorite, feldspar, magnetite, sulfides, barite, and REE-rich phases that include parisite, synchysite, bastnäsite, and monazite. Zones enriched in pyrochlore (the primary Nb host mineral) or

REE-phases occur quite sporadically in this unit. Apatite is either disseminated or occurs in narrow bands.

The magnetite beforsite consists of dolomite, magnetite, ilmenite, hematite, barite, and quartz, with variable amounts of rutile, apatite, fluorite, phlogopite, pyroxene, sulfides and pyrochlore. Much of the magnetite beforsite is brecciated, with magnetite beforsite occurring as clasts and/or as the matrix.

The barite beforsite is the least voluminous lithology. It consists of dolomite, barite, and quartz with minor or variable apatite, fluorite, phlogopite, pyroxene, feldspar, chlorite, sulfides, and contains the highest abundance of REE phases, which include parisite, synchysite, bastnäsite, and monazite. The barite beforsite primarily occurs as veins and dikes, a few millimeters to meters in width, but thicker zones (tens of meters thick) have been identified in a few cores.

Our work has documented a range in REE concentrations and patterns within the carbonatite. The chondrite-normalized REE patterns of apatite beforsite samples display a typical carbonatite pattern (Fig. 1) with moderate enrichment in the light REE (La 118-1780 ppm), no Eu anomaly, and a negative slope. Samples of apatite beforsite with the highest LREE content (>500 ppm La) contain late-stage fluorocarbonates (parisite, synchysite, and bastnäsite) and phosphates (monazite). The fluorocarbonates occur as clusters of fine needles, sometimes in a radiating morphology, which were first identified during the Molycorp exploration studies. Similarly, the monazite occurs as fine needles, in radiating or random orientations. The barite beforsite contains the most REE-rich zones within the Elk Creek carbonatite with La as much as 53,100 ppm, Ce as much as 66,900 ppm, and Nd as much as 13,100 ppm; their chondrite-normalized REE patterns display typical carbonatite REE patterns (Fig. 1). Similar to the apatite beforsite, samples of barite beforsite with the highest LREE content contain late-stage fluorocarbonates and phosphates (Fig. 2). The magnetite beforsite, the carbonatite unit that contains much of the Nb mineralization, has an anomalous REE pattern displaying enrichment of the more valued middle and heavy REEs (Eu, Gd, Tb, and Dy) relative to lower mass La, Ce, and Nd, and higher mass Tm, Yb, and Lu (Fig. 1). Studies are underway to determine the hosts of these elements in the magnetite beforsite.

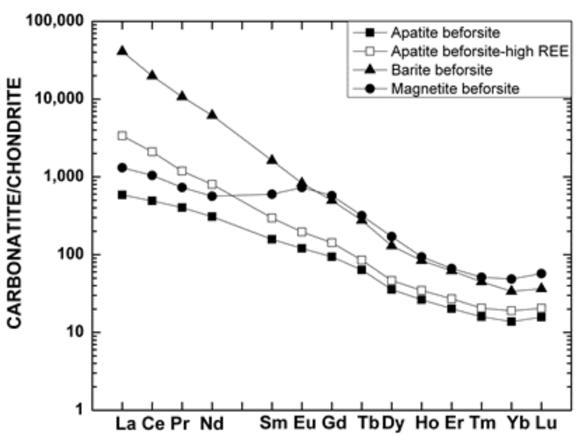

Figure 1. Chondrite-normalized REE diagram displaying various carbonatite lithologic units of the Elk Creek carbonatite. Median values used for apatite beforsite, apatite beforsite-high REE, barite beforsite, and magnetite beforsite.

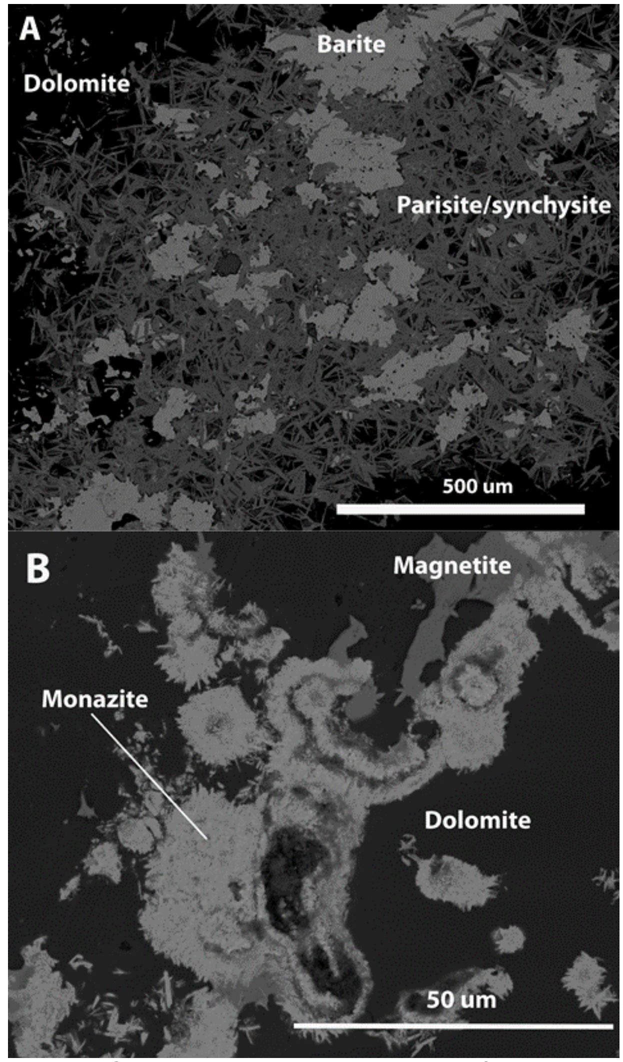

Figure 2. SEM backscattered electron images of REE phases in barite beforsite unit of Elk Creek carbonatite. A. REE fluorocarbonates. B. Monazite infilling in barite beforsite.

Detailed petrographic and scanning electron microscope (SEM) work have identified multiple generations of dolomite. The first generation (Dolomite I) is well crystalized and contains inclusions. It can be found intergrown with coarse apatite in apatite beforsite (Fig 3A). The apatite beforsite samples that contain only Dolomite I have lower REE concentrations than apatite beforsite samples that contain multiple generations of dolomite. Dolomite I also occurs in the magnetite beforsite where it is surrounded by a finer dolomite (Dolomite II; Fig 3B). Dolomite II is poorly crystalline and contains higher concentrations of Fe, Mn, and Sr than Dolomite I. A fine-grained dolomite, similar to Dolomite II, is the primary dolomite found in the barite beforsite.

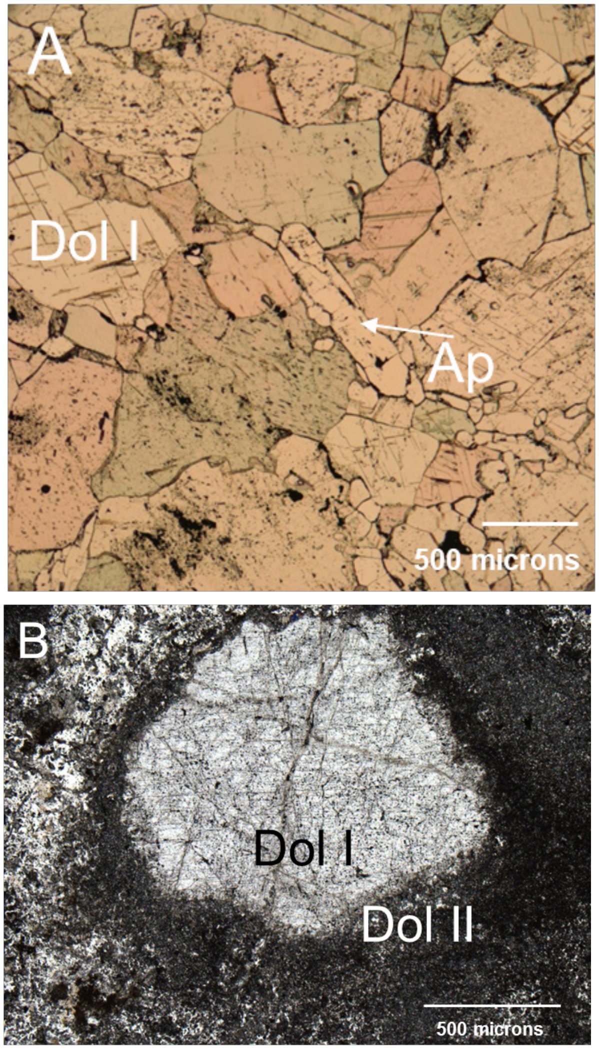

Figure 3. Photomicrographs displaying two generations of dolomite. A) coarse-grained apatite beforsite with Dolomite I. B) Magnetite beforsite with Dolomite I surrounded by Dolomite II.

3 Isotope geochemistry

Neodymium and strontium isotopes were used to evaluate the source of the REEs, the age of the carbonatite, and open-system behavior. Whole rock samples of each lithology were analyzed. The initial ε_{Ndi} (1.9 to 3.0, median of 2.4) is consistent with a lithospheric mantle source for the REEs. Sr_i values range from 0.70289 to 0.70748. The lower Sr_i values occur in the apatite beforsite and are consistent with a mantle reservoir, but the higher values suggest input from other sources including post-formation alteration (open-system behavior).

Because of the range in elemental concentrations of Sm and Nd, the Nd isotopic data can be used to calculate an age for the carbonatite (570±37 Ma). This age is similar to the few previously reported ages (~500-550 Ma (Carlson and Treves 2005). Furthermore, because the Nd isotopic data lie along a linear array, the REE ore had a single source.

Utilizing a micro drill on characterized billets, samples of various dolomites were obtained for calcium, oxygen, and strontium isotopic determinations. Carbon and oxygen isotope analyses of Dolomite I plot in or near the Primary Igneous Carbonate field, whereas Dolomite II extends to greater values ($\delta^{13}C$ to -1, $\delta^{18}O$ to 23) (Fig. 4). Dolomite II samples with the highest $\delta^{18}O$ and $\delta^{13}C$ values occur in zones of ferruginous alteration that resemble "rodbergite" as described at the Fen complex, Norway. These samples also have significantly higher Sr isotopic compositions, suggesting open system behavior; the timing of this event could be substantially later than the ore forming event.

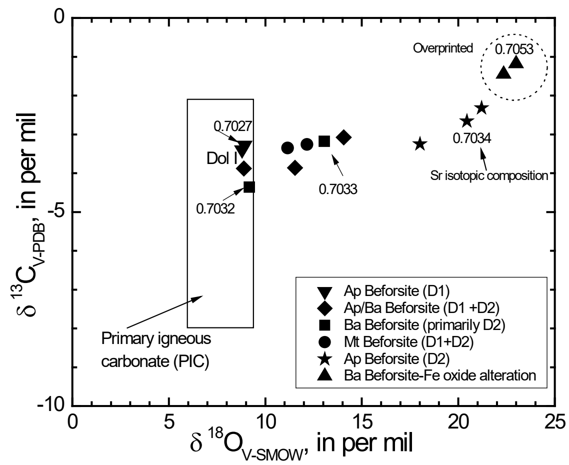

Figure 4. Variations in carbon and oxygen isotopic compositions of dolomite from various lithologies in the Elk Creek carbonatite with strontium isotopic values from the same aliquots. Ap=apatite, Ba=barite, Mt=magnetite, D1=Dolomite I, D2=Dolomite II. Field for primary igneous carbonate from Deines (1989).

Most of the Dolomite II samples lie along a trend away from the Primary Igneous Carbonate field and display a substantial increase in $\delta^{18}O$ (11 to 21) and only a slight increase in $\delta^{13}C$ (-3.5 to -2.5). This systematic variation could result from a decrease in temperature during crystallization or the input of fluids with higher $\delta^{18}O$ and $\delta^{13}C$ values. Because there is little change in the Sr isotopic compositions of the dolomites, open system behavior is less likely. This suggests that no external fluids are required to form the second generation dolomites.

4 Conclusions

Radiogenic and stable isotopic data on well-characterized samples can provide important constraints on ore-grade enrichment of REEs in carbonatites. Since Nd is an ore element, the Nd isotopic data provide direct information for the source of the ore. If there is sufficient Nd and Sm elemental concentration variation, then a carbonatite age can be calculated. If multiple ore forming events occur, Nd isotopic data can help determine if the Nd was derived from different sources, from the same source, or remobilized from within the carbonatite. The Sr isotopic data compliments the Nd but is more sensitive to later events. Many carbonatites display a range in Sr isotopic compositions suggesting that open system processes are common. This open system behavior may occur long after crystallization.

Stable isotopic data can provide additional insight into ore forming processes. C, O, and S can reside in ore and gangue minerals that form throughout the life of the deposit, and thus with well constrained samples, these data can provide important constraints on ore-grade enrichment processes.

Acknowledgements

This work was supported by the US Geological Survey's Mineral Resources Program (MRP), in part through the MRP External Research Program.

References

Carlson MP, Treves SB (2005) The Elk Creek Carbonatite, Southeast Nebraska-An overview. Natural Resources Research 14: 39-45

Deines P (1989) Stable isotope variations in carbonatites. In Bell K (ed) Carbonatites: Genesis and Evolution. Unwin Hyman, London, 301–359

Utilizing alteration (fenite) surrounding carbonatite intrusions as a REE and Nb exploration indicator

Holly A.L. Elliott, Sam Broom-Fendley, Frances Wall
Camborne School of Mines, University of Exeter, UK

Abstract. Carbonatites are the world's primary source of rare earth elements (REE) and niobium (Nb). China currently monopolizes the market, producing >95% of the world's supply. In order to meet UK government greenhouse gas emission targets, a reliable and sustainable supply of REE and Nb must be established in order to produce green technologies such as electric cars and wind turbines. The location of many carbonatite complexes are currently known, however the economic potential of few have been explored. Detailed petrological and geochemical analysis of fenite (metasomatic alteration surrounding carbonatite systems) has provided criteria to determine whether the source intrusion is enriched in these critical metals. Fenite micro-mineral assemblages enriched in REE and Nb indicate that the source of the fenitizing fluids is similarly enriched in these metals. Fenite apatite morphology and luminescence can also be used to indicate REE-enrichment in the source intrusion, showing systematic increases in Na, Sr and total REE (TREE) concentration from core to rim or homogenous late-stage crystals. These fenite alteration patterns are vertically and horizontally extensive, and can therefore be seen at a variety of erosion levels, providing a means of determining the economic potential of a system before undertaking expensive drilling campaigns.

1 Introduction

Carbonatites are often associated with high concentrations of a multitude of economically important minerals such as iron, copper, titanium, fluorite and uranium (Heinrich 1966; Mariano 1989; Pell 1996). In addition, carbonatites are the most important source of rare earth elements (REE) and niobium (Nb) (Wall 2014; Goodenough et al. 2016), both high profile critical metals considered imperative to technological advancement and the production of green technologies.

Despite the global distribution of both carbonatites and REE deposits, China currently produces >95% of the world's supply of REE (EC, 2017), causing vulnerability to future supply. REE are used in the production of neodymium-iron-boron magnets, which are important constituents of green technologies, such as electric cars and wind turbines. The UK government has recently committed to reducing greenhouse gas emission by at least 80% and ensuring every car and van is zero emission by 2050 (DTOLEV 2015; DBEIS 2018). Therefore, the future demand for REE is expected to increase dramatically (Yang et al. 2017).

Models relating to carbonatite and alkaline systems has not progressed considerably since that initially proposed by Le Bas (1977). However, this model has its limitations including lack of temporal relationships, ore formation processes and alteration. In order to ensure a sustainable and reliable source of REE for the future, new geomodels must be developed to enable exploration companies to better understand carbonatite systems and any critical metal-enrichments they contain.

2 Fenites and fenitization

Cooling and crystallizing carbonatite melts release multiple pulses of alkali-rich fluids (Morogan 1994; Le Bas 2008) which metasomatise the surrounding country rock during a process called fenitization. Traditionally, fenitization is considered to involve the addition of alkalis and the removal of silica (Brögger 1921; Bardina and Popv 1994). The resulting alteration is zoned both horizontally and vertically. A potassic fenite aureole which is typically brecciated and consists predominantly of alkali feldspar and metal oxides (Le Bas 2008; Doroshkevich et al. 2009) forms proximal to the intrusion, and a sodic fenite aureole characterized by veins of sodic pyroxenes and amphiboles forms distal to the intrusion.

3 Fenite as an exploration indicator

Until recently, the vast majority of research focused on carbonatite intrusions due to their economic importance, with fenite being relatively neglected in the literature. However, alteration patterns have been used with great success in the past to find other magmatic-related ore deposits such as porphyry copper (e.g. Sillitoe 2010). Fenite has the potential to be used in a similar way to explore for REE and Nb deposits.

3.1 Field relationships

Fenite aureoles form a distinct pattern of alteration that allows vectoring toward the source intrusion. The rocks themselves are easily recognizable in the field, without the need for expensive lab techniques. In addition, alteration can extend >1 km away from the source intrusion and can be exposed at a variety of erosion levels.

Evolution of carbonatitic magmas by fractional crystallization causes incompatible REE to be concentrated in later or last carbonatite differentiates (Heinrich 1966; Le Bas 1981; Wall 2014). Each phase of carbonatitic magmatism is associated with the release of fenitizing fluids, leading to multiple stages of fenitization which are represented as different assemblages or vein generations in the country rock. As such, the complexity of the fenite reflects magma evolution, and therefore the likelihood of REE-enrichment in the source intrusions.

Although brecciation is not recorded at every REE-rich carbonatite complex, there is a strong correlation between the presence of breccia and mineralization. Seventy percent of REE-enriched carbonatites are associated with brecciated fenite (Elliott et al. 2018), however the lack of observations at other sites may have been due to the literature focus or level of erosion. Widespread brecciation associated with carbonatite emplacement indicates the explosive release of fluids and volatiles from the evolving magma (Verplanck et al. 2014). The presence of these fluids and volatiles attest to the evolution and crystallization of the carbonatite magma, the same processes that concentrate incompatible REE in the residual melt, therefore it is logical that an association between brecciation and mineralization would exist.

3.2 Micro-mineral assemblages

Fenitizing fluids contain ligands such as chloride-, fluoride-, sulphate-, phosphate-, and/or carbonate anions, which can form complexes with REE and Nb, greatly enhancing their solubility in aqueous fluids (Andersen 1986; Haas et al. 1995; Williams-Jones et al. 2012; Tsay et al. 2014). Fenitizing fluids transport these critical metals into the surrounding fenite, where they precipitate as REE and Nb-enriched micro-mineral assemblages (Hogarth 2016; Bodeving et al. 2017; Dowman et al. 2017).

We have found micro-mineral assemblages enriched in REE and Nb globally (e.g. Songwe Hill, Malawi; Mountain Pass, USA; Sokli, Finland) and their presence in fenite could be used to determine the level of critical metal enrichment in the source intrusion.

3.3 Apatite characteristics

Apatite is a brilliant mineral for recording metasomatic activity, and the properties and composition of fluids (e.g. Harlov 2015). Apatite within fenite aureoles is typically zoned, fingerprinting the changing chemistry of multiple pulses of fenitizing fluids as the source intrusion evolves. Changes in chemical composition between these zones can be seen by contrasting luminescence colors under cold-cathodoluminescence (CL). Fenite apatite morphology and luminescence has been studied to investigate whether it can be used to determine if a carbonatite complex is REE-enriched.

4 Fenite apatite geochemical data

Fourteen carbonatite localities were selected, including REE-enriched and poor systems from US, Europe, Africa, and Asia. Fenite apatite was imaged used CL and then zones were analyzed for major element (using EPMA) and trace element (using LA-ICPMS) geochemistry.

Three main groups have been identified based on morphology and geochemical composition. Group 1 are concentrically zoned apatite. These can be found at both REE-enriched and poor complexes but with distinct differences. REE-poor systems display fenite apatite with

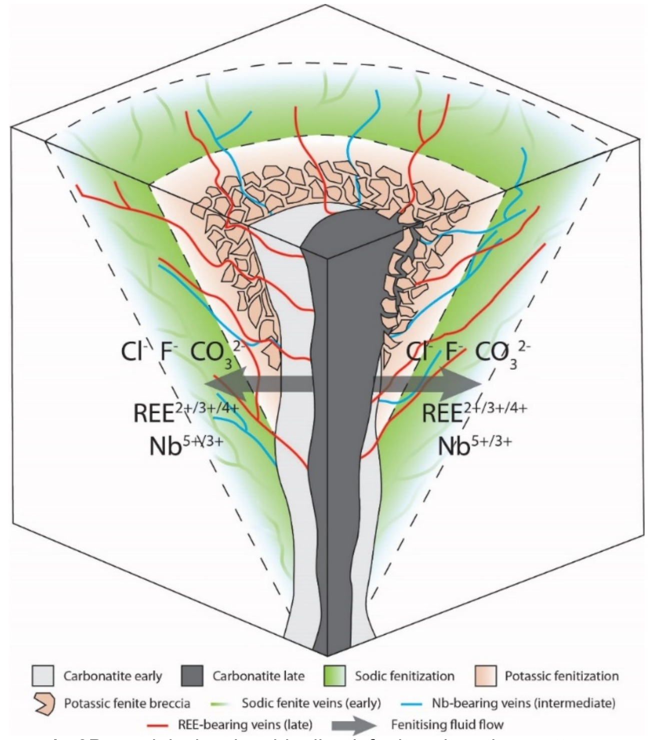

Figure 1. 3D model showing idealized fenite alteration patterns surrounding multiple generations of carbonatite intrusions. Fenitizing fluids contain ligands that mobilize Nb and REE into the surrounding fenite aureole. Adapted from Elliott et al. 2018.

unregimented zoning both between and within complexes. This is reflected in their chaotic composition, with no discernible trends. REE-enriched complexes displaying concentrically zoned apatite always have a core which luminesces green, rich in Mn and most likelyinherited from the protolith, surrounded by one or multiple purple luminescing rims. These crystals display increasing Na, Sr and total REE (TREE) concentration from core to rim.

Group 2 apatite are only found in fenite surrounding REE-enriched systems. These are late-stage and homogenous, displaying little to no variation in their blue-purple luminescence and are also enriched in Na, Sr, Th and TREE.

Group 3 apatite display evidence of hydrothermal alteration, such as being strung out by later veins, partial replacement by porous material or stringer textures with patchy luminescence. The composition of these crystals is variable, reflecting the hydrothermal alteration. However, this alteration can have the effect of preferentially mobilizing light REE (LREE).

5 Discussion

5.1 Utilizing fenite during exploration

Fenite alteration aureoles are easily identified by hand specimen in the field, allowing vectoring toward the source intrusion. However, if the source intrusion has not yet been exposed by erosion, it requires expensive drilling campaigns to determine any critical metal-enrichment present.

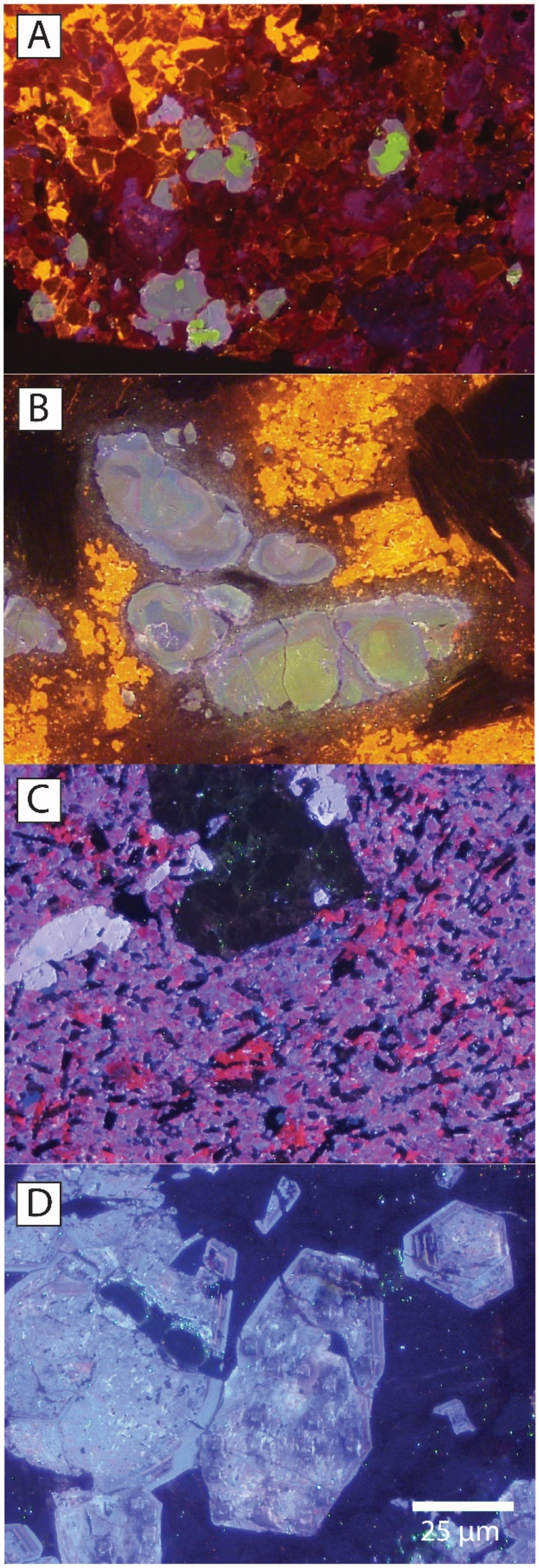

Figure 2. Cold cathodoluminesce images **A:** Group 1 apatite morphology from a REE-enriched complex showing green luminescing Mn-rich core surrounded by multiple purple luminescing REE-rich rims. Lofdal, Namibia. **B:** Group 1 apatite morphology from REE-poor complex showing unregimented layering. Tororo, Uganda. **C:** Group 2 apatite morphology showing homogenous blue-purple luminescing crystals. Mountain Pass, USA. **D:** Group 3 apatite morphology showing porous sponge-like alteration. Sokli, Finland.

Using the criteria outlined in this paper, provides the ability to use the fenite mineralogy as a means to determine whether further exploration of a site is warranted. The large vertical and horizontal extent of fenitization means that it can be exposed at a variety of erosion levels where an intrusion might not be. The presence of enriched micro-mineral assemblages and Group 1 and/or 2 apatite crystals can be used to indicate the enrichment of the source intrusion in REE and/or Nb.

5.2 Implications of hydrothermal alteration

Group 3 apatite display evidence of hydrothermal alteration, which can have the effect of preferentially mobilizing LREE, and concentrating HREE in the residual crystal. HREE-enrichment is rarer within carbonatite complexes and these elements are more valuable.

Spongey, porous crystals and stringer textures indicating the occurrence of hydrothermal alteration, have also been observed in intrusions at Songwe Hill, Kangankunde and Tundulu, Malawi (Broom-Fendley et al. 2016a; 2016b; 2017); Chipman Lake, Canada; and Sokli Finland (Chakmouradian et al. 2017). This indicates that although it is not currently considered economical to exploit metals from fenite aureoles, the alteration provides evidence for processes that are occurring inside the more economical carbonatite intrusion.

Acknowledgements

This research is part of the HiTech AlkCarb project which has received funding from the European Union's Horizon 2020 research and innovation programme under grant No 689909.

References

Andersen T (1986) Compositional variation of some rare earth minerals from the Fen complex (Telemark, SE Norway): implications for the mobility of rare earths in a carbonatite system. Min Mag 50: 503-509.

Bardina NY, Popov VS (1994) Fenites: systematics, formation conditions and significance for crustal magma genesis. Min Obsh 113:485-497.

Bodeving S, Williams-Jones AE, Swinden S (2017) Carbonate-silicate melt immiscibility, REE mineralizing fluids, and the evolution of the Lofdal intrusive suite, Namibia. Lithos 268: 268-271:383-398.

Brögger WG (1921) Die eruptivegestein des kristianiagebietes, IV. Das fengebiet in telemark. Norvegen. Naturv. Klasse 9:150–167.

Broom-Fendley S, Styles MT, Appleton D, Gunn G, Wall F (2016a) Evidence for dissolution-reprecipitation of apatite and preferential LREE mobility in carbonatite-derived late-stage hydrothermal processes. Amer Min 101:596-611.

Broom-Fendley S, Heaton T, Wall F, Gunn G (2016b) Tracing the fluid source of heavy REE mineralisation in carbonatites using a novel method of oxygen-isotope analysis in apatite: the examples of Songwe Hill, Malawi. Chem Geol 440: 275-287.

Broom-Fendley S, Brady AE, Wall F, Gunn G, Dawes W (2017) REE minerals at the Songwe Hill carbonatite, Malawi: HREE-enrichment in late-stage apatite. Ore Geol Reviews 81:23-41.

Chakhmouradian AR, Reguir EP, Zaitsev AN, Couëslan C et al (2017) Apatite in carbonatitic rocks: compositional variation, zoning, element partitioning and petrogenetic significance. Lithos 274-275:188-213.

Department for business, energy and industrial strategy (2018) Clean growth strategy executive summary. https://www.gov.uk/government/publications/clean-growth-strategy/clean-growth-strategy-executive-summary Accessed 15 September 2018.
Department for Transport, Office for Low Emission Vehicles (2015) http://webarchive.nationalarchives.gov.uk/20160805060601/https://www.gov.uk/government/news/uk-government-pledges-bold-ambition-for-electric-cars Accessed 15 September 2018.
Doroshkevich AG, Viladkar SG, Ripp GS, Burtseva MV (2009) Hydrothermal REE mineralization in the Amba Dongar carbonatite complex, Gujarat, India. Can Min 47:1105-1116.
Dowman E, Wall F, Treloar PJ, Rankin AH (2017) Rare earth mobility as a result of multiple phases of fluid activity in fenite around the Chilwa Island Carbonatite, Malawi. Min Mag 81:1367-1395.
Elliott HAL, Wall F, Chakmouradian AR et al (2018) Fenites associated with carbonatite complexes: a review. Ore Geol Reviews 93:38-59.
European Commission (2017) Study on the review of the list of critical raw materials. Criticality Assessments.
Goodenough KM, Schilling J, Jonsson E et al (2016) Europe's rare earth element resource potential: AN overview of REE metallogenic provinces and their geodynamic setting. Ore Geol Rev 72:838-856.
Haas JR, Shock, EL, Sassani DC (1995) Rare earth elements in hydrothermal systems: estimates of standard partial molal thermodynamic properties of aqueous complexes of the rare earth elements at high pressures and temperatures. Geochim Cosmochim Act 59:4329-4350.
Harlov DE (2015) Apatite: a fingerprint for metasomatic processes. Elements 11:171-176.
Heinrich EW (1966) The geology of carbonatites. Rand McNally & Company, Chicago.
Hogarth DD (2016) Chemical trends in the Meech Lake, Québec, carbonatites and fenites. Can Min 54:1105-1128.
Le Bas MJ (1977) Magmatic and metasomatic processes. In: Le Bas MJ (ed) Carbonatite-nephelinite volcanism: an African case history. John Wiley & Sons, pp 263-278.
Le Bas MJ (1981) Carbonatite magmas. Min Mag 44:133-140.
Le Bas MJ (2008) Fenites associated with carbonatites. Can Min 46:915-932.
Mariano AN (1989) Nature of economic mineralization in carbonatite and related rocks. In: Bell K (ed) Carbonatites: genesis and evolution. Unwin Hyman, pp 149-176.
Morogan V (1994) Ijolite versus carbonatite as sources of fenitization. Terra Nova 6:166-176.
Pell J (1996) Mineral deposits associated with carbonatites and related alkaline igneous rocks. In: Mitchell RH (ed) Undersaturated alkaline rocks: mineralogy, petrogenesis, and economic potential. No. 24 in Mineralogical Association of Canada Short Course Series. Min Assoc Can, pp 271-310.
Sillitoe RH (2010) Porphyry copper systmes. Econ Geol 105:3-41.
Tsay A, Zajacz Z, Sanchez-Valle C (2014) Efficient mobilization and fractionation of rare-earth elements by aqueous fluids upon slab dehydration. Earth Planet Sci Lett 398: 101-112.
Verplanck PJ, Van Gosen BS, Seal RR, McCafferty AE (2014) A deposit model for carbonatite and peralkaline intrusion-related rare earth element deposits. In: Mineral Deposit Models for Resource Assessment. No. 2010-5070-J in Scientific Investigations. US Geological Survey, pp 1-58.
Wall F (2014) Rare earth elements. In: Gunn G (ed) Critical Metals Handbook. John Wiley & Sons, pp 312-339.
Williams-Jones A, Migdisov AA, Samson I (2012) Hydrothermal mobilization of the rare earth elements: a tale of "Ceria" and "Yttria". Elements 8: 355-360.
Yang Y, Walton A, Sheridan R et al (2017) REE recovery from end-of-life NdFeB permanent magnet scrap: a critical review. J Sustain Metall 3:122-149.

Ore geometry and emplacement style of the carbonatite-hosted Morro do Padre Nb deposit

Matheus Palmieri[1], José A. Brod[2], Pedro F. O. Cordeiro[3], José C. Gaspar[4], Paulo A. R. Barbosa, Tereza C. Junqueira-Brod[2], Sergio A. Machado[5], Bruno P. Milanezi[5], Luis C. Assis
[1]*Centro de Desenvolvimento de Tecnologia Nuclear*
[2]*Universidade Federal de Goiás*
[3]*Pontificia Universidad Católica de Chile*
[4] *Universidade de Brasília*
[5]*CMOC International Brasil*

Abstract. The Morro do Padre niobium deposit contains important unexploited niobium resources within carbonatite-associated rocks and laterites of the Catalão II complex, Brazil. The deposit can be divided into three zones: a) The Lower Hypogene Zone; b) The Upper Hypogene Zone; c) The Laterite Zone. The Hypogene Zone is defined by dike swarms of nelsonites (magnetite-apatite-carbonate-phlogopite-pyrochlore rocks) and carbonatites cutting country rocks. Two main nelsonite phases occur: i) the N1 apatite-rich nelsonites and ii) the N2 magnetite-rich nelsonites. Additionally, two carbonatite phases are recognized: C1 calcite carbonatite and C2 dolomite carbonatite. The hypogene mineralization is defined by the abundance of nelsonite dikes, particularly N2, which are modally rich in pyrochlore. 3D modelling based on the drill hole database suggests a general EW elongated, pipe-like shape for these intrusions which, unlike other examples in the province, are not intruded directly into a coeval alkaline silicate plutonic series. This can be readily explained by the Morro do Padre deposit representing the emplacement of nelsonite and carbonatite dikes in the roof of a larger carbonatite complex.

1 Introduction

Carbonatite complexes containing phoscorite rocks (magnetite-apatite-olivine) are rare in the geological record, with only around 20 occurrences known worldwide (Krasnova et al. 2004; Wall and Zaitsev 2004). They are, however, extremely relevant as mineralizing systems, since igneous complexes containing associations of phoscorite, carbonatite, and alkaline silicate rocks have a strong potential for ore deposits. These include a wide variety of mineralization styles such as P, Nb, Cu, REE, Ba, Ti, vermiculite and lime, among others. The majority of the world's production of Nb comes from carbonatite complexes, particularly those in the Alto Paranaíba Igneous Province (APIP), in Brazil. The two biggest sources of production are mines in giant reserves in the Araxá complex (Gierth and Baecker 1986; Issa Filho et al. 1984) and smaller deposits in the Catalão I complex (Cordeiro et al. 2011) and Catalão II complex (Palmieri et al. in submission). Together, these deposits represent ca. 85% of the global niobium production (Mitchell et al. 2015).

In spite of having been mined for more than 40 years, ore formation processes associated with these carbonatite-hosted niobium deposits have not been satisfactorily explained in comparison to processes observed in other well-known Nb-barren carbonatite complexes.

This work is part of a larger research to be submitted for publication covering a systematic study of ore geometry, paragenetic sequences, mineral chemistry and lateritization in Morro do Padre. The aim is to understand what makes these APIP carbonatites highly fertile for niobium mineralization and provide information to help build both advanced exploration models and refined ore processing technologies. To address this, we present a discussion on the structure and mineralization styles of the hypogene deposit of Morro do Padre on the basis of geophysical and ore modelling data. Our goal is to provide a complete emplacement model that takes into account the time-space evolution of this mineralizing system.

2 The Alto Paranaíba Igneous Province (APIP)

The Late-Cretaceous alkaline rocks of southern Goiás and western Minas Gerais states, in central Brazil, spread over an area of 25,000 km^2 and have been grouped under the designation of Alto Paranaíba Igneous Province, APIP, by Gibson et al. (1995). The province consists mainly of kamafugitic lavas and plugs, with subordinate kimberlite and lamproite diatremes and alkaline-carbonatite plutonic complexes. This extensive magmatic activity is interpreted as the result of the impact of the Trindade mantle plume head under central Brazil, at ca. 90 Ma, which melted the overlying metasomatized sub-continental lithospheric mantle to produce voluminous ultrapotassic magmas (Thompson et al. 1998). In spite of the wide range of rock types, the carbonatite complexes in the APIP have a strong ultrapotassic character and kamafugitic affinity. They are also co-genetic with numerous small kamafugite pipes occurring throughout the province and with kamafugite lavas and pyroclastics of the Mata da Corda Group (Araujo et al. 2001). The chronological, spatial and petrological affinity of kamafugites and carbonatites led Brod et al. (2000) to propose that they derived from the same parental melt.

3 The Morro do Padre deposit

The Morro do Padre Niobium deposit is hosted in the southern part of Catalão II, an APIP carbonatite complex in the state of Goiás. Along with the Boa Vista Nb deposit, 100 m to the west, Morro do Padre is represented by dike swarms of carbonatites and magnetite-apatite rocks (Figure 2), named here as nelsonite (Yegorov 1993) emplaced within fenitized Precambrian phyllites and amphibolites. The northern part of the Catalão II complex, on the other hand, resembles the other APIP complexes which can be roughly depicted as an outer silicate plutonic series and an inner carbonatite-phoscorite core.

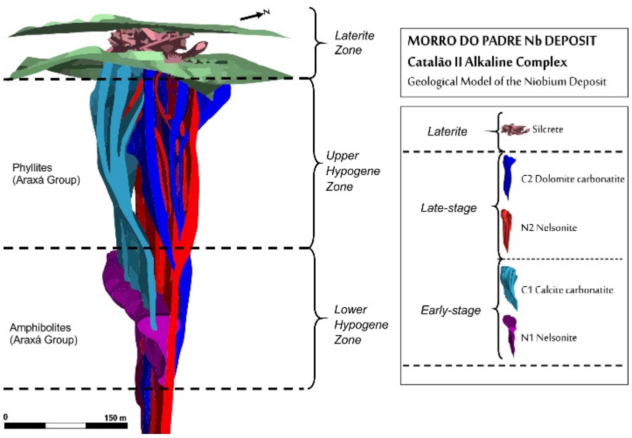

Figure 1. Geological model of the Morro do Padre Nb deposit and associated lithologies (Palmieri 2011).

On the basis of currently available drill core information and for modelling purposes, we subdivided the deposit into three distinct vertical sections from bottom to top into the Lower Hypogene Zone, the Upper Hypogene Zone and the Laterite Zone.

The hypogene ore is characterized by a complex system of crosscutting dikes of pyrochlore-bearing carbonatites and nelsonites hosted within country-rock phyllites and amphibolites. The general envelope of the hypogene ore reveals an E-W trend due to a dominant regional country rock fracture system, which albeit not the most pervasive, is also observable in regional magnetometry and satellite images (Palmieri 2011). The laterite ore developed over these fresh rocks through pedogenetic processes and compounded their mineralogical and textural complexity. The relationships between nelsonite-, carbonatite- and country rock-dominated units in the Upper Hypogene Zone of the Morro do Padre deposit are shown in Figure 1. Note that the geological units depicted in the model represent zones of high abundance of nelsonite and carbonatite, rather than continuous igneous bodies. Separation of hypogene and laterite ore zones is important for mining and ore processing because these ores have different geometallurgical behavior (e.g. Ribeiro 2008).

The Lower Hypogene Zone is 400 m wide and it was intercepted from 460 to 600 m of depth, where drilling ended. This zone is dominated by horizontally layered calcite-carbonatites (C1) and nelsonites (N1) hosted by fenitized amphibolites of the Neoproterozoic basement. N1 nelsonites occur in this zone as rhythmic layers of apatite-nelsonite and pegmatoidal nelsonite. The Lower Hypogene Zone is cut by late-stage nelsonite (N2) and dolomite carbonatite dikes that proceed upwards to define the Upper Hypogene Zone.

The Upper Hypogene Zone is roughly 400 m thick and 140 m wide, but unlike its lower counterpart, it is dominated by stockworks of crosscutting pyrochlore-bearing nelsonite (N2), dolomite carbonatite and calcite-carbonatite dikes (usually a few centimeters thick, more rarely up to 1-2 m), with minor syenite and pyroxenite. These dikes cut fenitized Precambrian phyllites and subordinately amphibolites and quartzites, of the Brasília Belt.

The Laterite Zone is 470 m long, 160 m wide and represents the relatively thin (75 m) upper part of the Morro do Padre deposit. This zone poses additional challenges to the understanding and modeling of the mineralization because ores may have inherited the heterogeneity from primary mineralization but were overprinted by variable degrees of complex soil formation processes, up to near obliteration of primary hypogene features. Thus, unlike the hypogene ore, this zone is horizontally divided based on mineralogical and chemical characterization, from base to top into the Micaceous Ore, the Silcrete Ore and the Kaolinite-Oxide Ore.

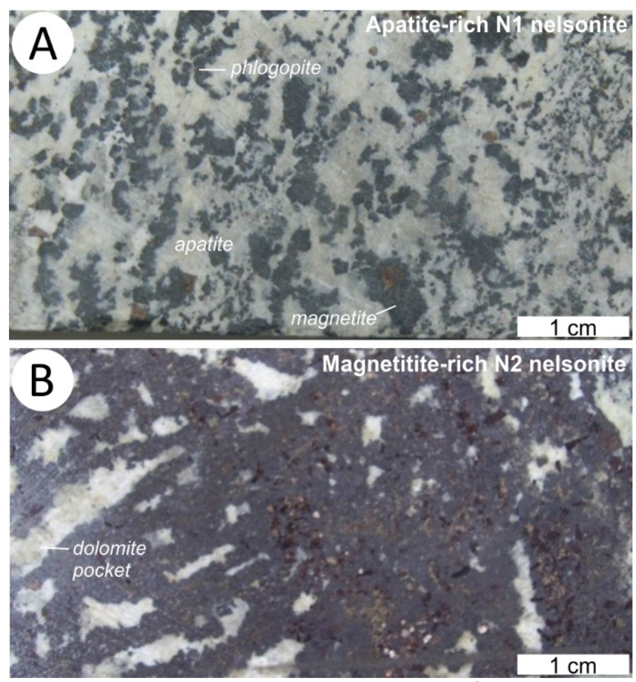

Figure 2. Pyrochlore-bearing nelsonite samples from the Morro do Padre Deposit **a.** Apatite-rich N1 nelsonite; **b.** Magnetite-rich N2 nelsonite with dolomite pockets (Palmieri 2011).

4 Discussion

The Morro do Padre deposit is hosted in the southern part of the Catalão II complex, a carbonatite complex that was poorly known until Palmieri (2011) reported on exploration efforts performed in the last 20 years. Field and core logging observations and geophysical data (Fig. 3), collected during multiple exploration campaigns, indicate that Catalão II is, in fact, comprised of two main intrusions: a southern one, which hosts the Morro do Padre deposit, and a northern one. Both of them show carbonatite-related rocks but with wide variation of emplacement styles that can be explained by emplacement at different depths or levels of the intrusive system.

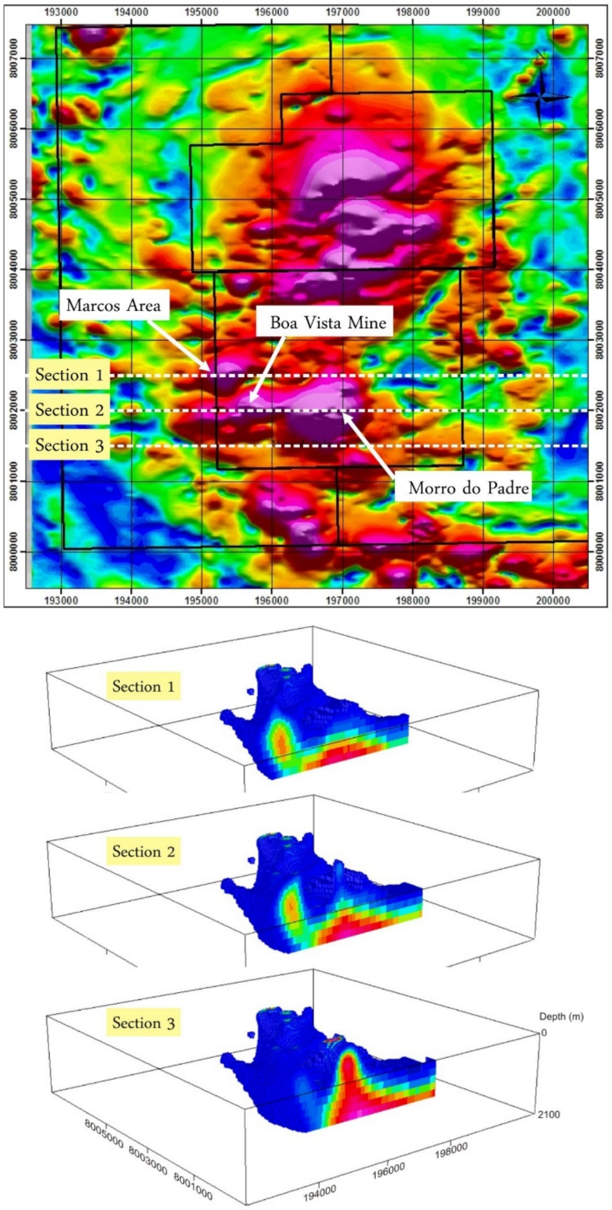

Figure 3. Analytical signal image of the Catalão I complex and magnetic modelling of the southern part of Catalão II, where the Morro do Padre Nb deposit is hosted (Palmieri 2011).

The northern part of Catalão II is a concentric, layered intrusion with an outer ultramafic rim and a phoscorite-carbonatite core as multiple intrusions, akin to other APIP complexes such as Tapira and Salitre (Brod et al. 2013; Barbosa et al. 2012), and constitutes the core of the carbonatite complex system. The southern part of Catalão II, on the other hand, is represented by nelsonite and carbonatite dikes cutting metasedimentary basement rocks and could be interpreted as the roof of a deeper former pluton.

Geophysical modelling contributes to the suggestion of a deeper and larger magma chamber below 1000 m, at depths not yet reached by drilling (Fig. 3). In this model, the magnetic anomalies represented at surface by the nelsonite dikes that define the Morro do Padre and Boa Vista Nb deposits are rooted in a deeper magnetic anomaly.

Some fundamental differences between these two deposits, however, must be highlighted. The Morro do Padre hypogene zone has abundant carbonatites (C1 and C2) along with N1 and N2 nelsonites, rendering country rocks subordinate, although still present, in the mineralized section . In the Boa Vista Mine, on the other hand, carbonatite and nelsonite dikes are more scattered, implying not only a volumetrically more important contribution of barren metavolcanics and metasedimentary country rocks, but also a variation of emplacement level/depth between them, with the Boa Vista Mine representing a higher intrusive level, compared with the Morro do Padre deposit.

4.1 Emplacement styles

Within Morro do Padre, vertical lithological zoning of the hypogene zone can be indicative of the mode of emplacement of these magmas at different depths. The Lower Hypogene Zone, for example, can be interpreted as the result of the infilling of a small chamber or sill at the contact between amphibolite and quartzite country rocks. Such a contact zone would be prone to allow for magmas to pond and undergo several stages of differentiation and recharge, producing horizontal cyclic units which characterize the deeper part of Morro do Padre.

The Upper Hypogene Zone, on the other hand, would start to form with the ascension of C1 carbonatite magma upwards through quartzite country rocks. As suggested by crosscutting relationships, the entire system would be later cut by magmas that crystallized into the N2 nelsonites and C2 carbonatite, therefore implying that N2 and C2 represent a later stage in the evolution of the complex. It is noteworthy that both the carbonatite and nelsonite units tend to splay upward, suggesting that lower lithostatic pressure at the higher parts of the structure allowed a larger number of open fractures to be permeated by magmas.

These textural and lithological zoning features imply that magmas responsible for Morro do Padre percolated unusually during their ascension. Similarly, to pure carbonatite magmas whose fundamental structural units lack the ability to polymerize (Treiman 1989), the magmas responsible for originating the Morro do Padre niobium deposit emplaced as thin dikes, which is consistent with very low viscosity. Such extremely low-SiO_2, low-viscosity liquids are incapable of forcing their intrusion and forming large massive igneous bodies showing instead, a rather “runny” behavior, seeping through existing fractures with ease. This behavior implies that a given magma (e.g. a carbonatite or a nelsonite) will intrude as a zone of parallel and braided thin dikes rather than as a single body. An important consequence of this feature is to render the mapping of individual dikes ineffective in any useful scale. These features, in association with small magma volumes and the configuration and structures of the wall rocks, lead to their emplacement as multiple phases of vertical or sub-vertical swarms of thin dikes and veins, rather than as massive bodies.

5 Implications

The majority of the hypogene mineralization in Morro do Padre is given by the abundance of N2 dikes, which are modally rich in pyrochlore and that, together with C2 dolomite carbonatites, comprise the latest stage of the evolution of Morro do Padre. The genesis of such magnetite-apatite rich rocks, however, remains a matter of debate given the importance of liquid immiscibility in carbonatite systems. In the case of N2 and C2, which appear to be coeval, it is not clear whether they are a pair of magmas related by liquid immiscibility or two stages of a single crystal fractionation process. Recent experimental and melt inclusions work support the existence of iron melts able to explain 'iron lavas' from El Laco and other cordilleran equivalents (Tornos et al 2016). An oxide-phosphate melt would be able to explain the occurrence of nelsonite and phoscorite dikes in the APIP, however, evidence for such melts is still largely textural (dike emplacement and nelsonite pockets/droplets within carbonatites and vice-versa). On the other hand, the textural features depicted in figure 2 suggest that the N1 sample has an equigranular texture (Fig. 2a) that could easily be produced by *in-situ* crystallization from either a phosphate-oxide or carbonatite magma, but N2 (Fig. 2b) could be explained as accumulations on a carbonatite dike wall. The suggested alternatives are not mutually exclusive, so the interplay between carbonatite and nelsonite magmas in Catalão II, in general and as a niobium ore formation process merits further petrological research is needed to test the relative role of the various differentiation processes involved.

Acknowledgements

This work was supported by CNPq - Brazilian Council for Research and Development (Grants 480259/2009-7 - Universal; 550376/2010-0 - CT-Mineral and 306650/2007-0) and Anglo-American Brazil (Mineração Catalão and Copebrás), for which the authors are most grateful.

References

Araujo ALN, Carlson RW, Gaspar JC, Bizzi LA (2001) Petrology of kamafugites and kimberlites from the Alto Paranaíba Alkaline Province, Minas Gerais, Brazil. Contrib to Mineral Petrol 142:163–177.

Barbosa ESR, Brod JA, Junqueira-Brod TC, Dantas EL, Cordeiro PFO, Gomide CS (2012) Bebedourite from its type area (Salitre I complex): A key petrogenetic series in the Late-Cretaceous Alto Paranaíba kamafugite-carbonatite-phoscorite association, Central Brazil. Lithos 144–145:56–72.

Brod JA, Gibson SA, Thompson RN, Junqueira-Brod TC, Seer HJ, Moraes LC, Boaventura GR (2000) The Kamafugite-Carbonatite association in the Alto Paranaíba Igneous Province (APIP) Southeastern Brazil. Brazilian J Geol 30:408–412.

Brod JA, Junqueira-Brod TC, Gaspar JC, Petrinovic IA, Valente SC, Corval A (2013) Decoupling of paired elements, crossover REE patterns, and mirrored spider diagrams: Fingerprinting liquid immiscibility in the Tapira alkaline-carbonatite complex, SE Brazil. J South Am Earth Sci 41:41-56.

Cordeiro PFO, Brod JA, Palmieri M, Oliveira CG, Barbosa ESR, Santos RV, Gaspar JC, Assis LC (2011) The Catalão I niobium deposit, central Brazil: Resources, geology and pyrochlore chemistry. Ore Geol Rev 41:112–121.

Gibson SA, Thompson RN, Leonardos OH, Dickin AP, Mitchell JG (1995) The late cretaceous impact of the trindade mantle plume: Evidence from large-volume, mafic, potassic magmatism in SE Brazil. J Petrol 36:189–229.

Gierth E, Baecker ML (1986) A mineralização de nióbio e as rochas alcalinas associadas no complexo Catalão I, in: Schobbenhaus, C. (Ed.), Principais Depósitos Minerais Do Brasil. MME/DNPM, Brasília, 456–462.

Issa Filho A, Lima PRAS, Souza OM (1984) Aspectos da geologia do complexo carbonatítico do Barreiro, Araxá, MG, Brasil, in: CBMM (Ed.), Complexos Carbonatiticos Do Brasil: Geologia. CBMM, São Paulo, 20–44.

Krasnova NI, Petrov TG, Balaganskaya EG, Garcia D, Moutte D, Zaitsev AN, Wall F (2004) Introduction to phoscorites: occurrence, composition, nomenclature and petrogenesis. In: Wall, F., Zaitsev, A.N. (Eds.), Phoscorites and Carbonatites from Mantle to Mine: the Key Example of the Kola Alkaline Province. Mineralogical Society Series, London, 45–79.

Mitchell, R. H., 2015. Primary and secondary niobium mineral deposits associated with carbonatites. Ore Geology Reviews, 64:626-641.

Palmieri, M., 2011. Modelo Geológico e Avaliacão de Recursos Minerais do Depósito de Nióbio Morro do Padre, Complexo Alcalino-carbonatítico Catalão II, GO. Universidade de Brasília.

Ribeiro CC (2008) Geologia, Geometalurgia, Controles e Gênese dos depósitos de fósforo, terras raras e titânio do Complexo Carbonatítico Catalão I, GO. Universidade de Brasília.

Tornos F, Velasco F, Hanchar JM (2016) Iron-rich melts, magmatic magnetite, and superheated hydrothermal systems: The El Laco deposit, Chile. Geology 44:427–430.

Thompson RN, Gibson SA, Mitchell JG, Dickin AP, Leonardos OH, Brod JA, Greenwood JG (1998) Migrating Cretaceous-Eocene magmatism in the Serra do Mar Alkaline Province, SE Brazil: melts from the deflected Trindade mantle plume? J Petrol 39:1493–1526.

Treiman AH (1989) Carbonatite magma: properties and processes, in: Bell, K. (Ed.), Carbonatites: Genesis and Evolution. Unwin Hyman, London, 89–104.

Wall F, Zaitsev AN (2004) Phoscorites and Carbonatites from Mantle to Mine: the Key Example of the Kola Alkaline Province. Mineralogical Society Series 10, London.

Yegorov LS (1993) Phoscorites of the Maymecha–Kotuy ijolite–carbonatite association. Int Geol Rev 35:346–358.

The giant Bayan Obo REE-Nb-Fe deposit, China: How did it come into being?

Hong-Rui Fan[1,2], Kui-Fang Yang[1,2], Fang-Fang Hu[1,2], Shang-Liu[1,2]
1. Key Laboratory of Mineral Resources, Institute of Geology and Geophysics, Chinese Academy of Sciences, China
2. College of Earth Science, University of Chinese Academy of Sciences, China

Abstract. The world's largest Bayan Obo REE deposit is hosted in the massive dolomite, and nearly one hundred carbonatite dykes occur in the vicinity of the deposit. The carbonatite dykes, corresponding to different evolutionary stages of carbonatite magmatism, can be divided into three types: dolomite, co-existing dolomite-calcite and calcite. The latter always has the highest REE content. The ore-hosting coarse-grained dolomite represents a Mesoproterozoic carbonatite pluton and the fine-grained dolomite resulted from the extensive REE mineralization and modification of the coarse-grained variety. The first episode mineralization is characterized by disseminated mineralization in the dolomite. The second or main-episode is banded and/or massive mineralization, cut by the third episode consisting of aegirine-rich veins. The mineralization is rather variable with two peaks at ~1400 Ma and 440 Ma. The early peak corresponds in time to the intrusion of carbonatite dykes. The later significant thermal event resulted in the formation of late-stage veins. Bayan Obo deposit is a product of mantle-derived carbonatitic magmatism, which was likely related to the breakup of Columbia. Some remobilization of REE occurred due to subduction of the Palaeo-Asian oceanic plate during the Silurian.

1 Introduction

Bayan Obo is the largest rare earth element (REE) ore deposit and the second largest niobium deposit in the world, and also a large iron ore deposit in China. More than 80% of the REE resources in China are situated int Bayan Obo region. Since the discoveries of Fe ores in the Main Orebody in 1927 by Mr. Daoheng Ding and REE minerals in 1935 by Mr. Zuolin He at Bayan Obo, many studies have been carried out, particularly in the last two decades, on the geological background, mineral constituents, geochronology and geochemistry. However, owing to the complicated element/mineral compositions and the occurrence of several geological events at Bayan Obo, the genesis of this giant REE ore deposit, including its potential ore-forming sources, particularly with regard to the mechanism of REE enrichment, still remains subject to intense debate.

2 Regional and ore geology

The Bayan Obo deposit is located approximately 90 km south of the China and Mongolia border, at the northern margin of the North China Craton (NCC), bordering the Central Asian Orogenic Belt to the north. Gentle fold structures, composed mostly of the low grade metasedimentary units of the Mesoproterozoic Bayan Obo Group, are distributed from south to north in the region. The deposit, hosted in massive dolomite, occurs in one of the syncline cores. To the north of the ore body, a complete sequence of the Bayan Obo Group is exposed in the Kuangou anticline, which is developed on Paleoproterozoic basement rocks with a distinct angular unconformity. The low grade clastic sequences of the Bayan Obo Group represent the sedimentary units deposited within the Bayan Obo marginal rift, which correlates with the Mesoproterozoic continental breakup event of the NCC. The ore-hosting dolomites, covered by K-rich slate, extending 18 km from east to west and approximately 2 km wide, were once considered as a component of Bayan Obo Group. The origin of the dolomites is still disputed, with proposals for both sedimentary or carbonatite-related origins.

Basement rocks at Bayan Obo are composed of Neoarchean mylonitic granite-gneiss (2588±15Ma), Paleoproterozoic syenite and granodiorite (2018±15Ma), and biotite granite-gneiss and garnet-bearing granite-gneiss (~1890 Ma). Dioritic-granitic plutons, composed of gabbro, gabbroic diorite, granitic diorite, adamellite, and biotite granite, are distributed within a large area in the south and east Bayan Obo mine. These plutons were once regarded as intruding from Devonian to Jurassic. New geochronology data reveal that these plutons were formed in a post-collisional tectonic regime at convergent margins in the late Paleozoic in a narrow time interval from 263 to 281 Ma, with a peak age of 269 Ma, consistent with plate subduction during the closure of the Palaeo-Asian Ocean. It has been proved that REE mineralization at Bayan Obo has no direct relationship with these late Paleozoic granitoids.

REE reserves at Bayan Obo are 57.4 million metric tons (Mt) with an average grade of 6% RE2O3. Niobium reserves are estimated at 2.2 Mt with an average grade of 0.13% Nb_2O_5, and total Fe reserves are at least 1500 Mt with an average grade of 35%. REEs in the ores are rich in LREE, mostly are Ce, La and Nd, which occupy >90% LREE. There are nearly one hundred carbonatite dykes at Bayan Obo, intruded into the basement rocks and/or the Bayan Obo Group. The dykes are usually 0.5 to 2.0 m wide, 10 to 200 m long, and strike generally to the northeast or northwest. It is significant that some dykes have metasomatised the country rocks on both sides of the contact zones, producing fenites characterized by the presence of sodic amphiboles and albite. The major constituent minerals in the dykes are dolomite and calcite, which are associated with subordinate apatite, monazite, barite, bastnäsite, and magnetite. The REE contents in the different carbonatite dykes vary from ca. 0.02 to ca. 20 wt%.

The mine is composed of three major ore bodies: the East, Main and West Orebodies. Relative to the West Orebody, the East and Main Orebodies occur as larger lenses, underwent more intense fluoritization, fenitization and hosted more abundant REE and Nb mineralization. Fluorite appears in the fenitized dolomite, and riebeckite and phlogopite are observed in the K-rich slate. The REE ores are defined to be four types, namely the riebeckite, aegirine, massive, and banded types. The principal REE minerals are bastnäsite-(Ce) and monazite-(Ce), and are accompanied by various REE and Nb minerals, such as huanghoite, aeschynite-(Ce), fergusonite, and columbite. The iron minerals are magnetite and hematite. The main gangue minerals include fluorite, barite, alkali amphibole, apatite, quartz and aegirine.

Based on ore occurrences and crosscutting relations, three important REE mineralizing episodes can be indentified at the simplest level. The first episode is characterized by disseminated mineralization, which contains monazite associated with ferroan dolomite, ankerite and magnetite, concentrated along fractures and grain boundaries in the relatively unaltered/massive dolomite. The second or main-episode is banded and/or massive mineralization, which shows a generalized paragenetic sequence of strongly banded REE and Fe ores showing alteration to aegirine, fluorite and minor alkali amphibole. The banded and massive ores are cut by the third episode consisting of aegirine-rich veins containing coarser crystal fluorite, huanghoite, albite, calcite, biotite, and/or pyrite.

3 Genesis of carbonatite dyke and ore-hosting dolomite

Abundant carbonatite dykes occur adjacent to the eastern and southern of the Bayan Obo mine and particularly within the Kuangou anticline. The dykes can be divided into three types: dolomite, co-existing dolomite-calcite and calcite type, corresponding with different evolutionary stages of carbonatitic magmatism. The latter always has higher REE content. Field evidence of incision contact shows that a dolomite carbonatite dyke was cut by a calcite one, showing that the emplacement of the calcite dyke is later than the dolomite one. Geochemical data show that Sr and LREE contents in the dykes gradually increase from dolomite type, through calcite-dolomite type, to calcite type. This trend might be resulted from the crystal fractionation of a carbonatitic magma.

The origin of the ore-hosting dolomite at Bayan Obo has been addressed in various models, ranging from a normal sedimentary carbonate rocks to volcano-sedimentary sequence, and a large carbonatitic intrusion. All arguments have been supported with reference to the trace element and isotopic composition of the dolomite. Based on elemental geochemistry, and C, O, and Mg isotopic geochemistry, the ore-hosting dolomites are strongly enriched in LREEs, Ba, Th, Nb, Pb, and Sr, and have very different (PAAS)-normalized REE patterns. The evidence obtained shows that the ore-hosting dolomite at Bayan Obo was mainly derived from the mantle (Yang et al., 2011).

A relatively small volume of coarse-grained dolomite occurs at Bayan Obo mainly in the West Orebody, as well as in the northern part of the Main Orebody. The rocks are composed predominantly of coarse-grained euhedral–subhedral dolomite, associated with evenly distributed fine-grained apatite, magnetite, and monazite. The fine-grained dolomites are distributed widely and constitute the main part of the deposit. They commonly also appear massive in outcrop and consist predominantly of dolomite or ankerite, which is mostly fine-grained, ranging from 0.05mm to 0.1 mm in diameter. The coarse-grained and fine-grained facies of the dolomite occurring at Bayan Obo introduced additional complexities into the interpretation of their genesis.

Field observations in the northern part of the Main Orebody revealed that the coarse-grained dolomite intruded into the Bayan Obo group quartz sandstone as apophyses. However, the geochemical characteristics of the coarse-grained dolomite are not consistent with those of the fine-grained dolomite. The major and trace element contents of the coarse-grained dolomite are very similar to the calcite-dolomite carbonatite dykes at Bayan Obo. Data from those samples overlap within the magnesio-carbonatite region on the CaO-MgO-(FeO+Fe_2O_3+MnO) classification diagram, and show similar REE contents and distribution patterns on a chondrite-normalized abundance diagram. The similar geochemical characteristics of coarse-grained dolomite and calcite-dolomite carbonatite dykes, and the intrusive contact between the coarse-grained dolomite and wallrocks, indicate that the coarse-grained dolomite is likely an earlier phase of calcite-dolomite carbonatite stock, which did not witness the subsequent mineralization event from the residual carbonatitic melts, probably because it is located far from the main mineralized zone. The fine-grained dolomite from the Main, East and West Orebody differs from the coarse-grained dolomite in their major, trace element and REE characteristics. The fine-grained dolomite shows major element compositions comparable to that of the dolomite carbonatite dykes. All the samples fall in the field of dolomite carbonatite dykes on the CaO-MgO-(FeO+Fe_2O_3+MnO) classification diagram. The REE content and distribution patterns of the fine-grained dolomite samples, however, are similar to those of the calcite carbonatite dykes.

The REE content in the dolomite carbonatite dykes is relatively low, as compared to the extreme accumulation in the calcite carbonatite dykes at Bayan Obo. It is noted that the REE minerals in the fine-grained dolomite occur as ribbons or aggregates. It has been found that the REE minerals are distributed around dolomite phenocrysts in the fine-grained dolomite and, therefore, formed. These observations lead us to believe that the fine-grained dolomite represents an early stage large-scale dolomite carbonatite pluton, and the superposed REE mineralization was derived from the later calcite carbonatite magma.

4 REE mineralizing time

According to the occurrences of rocks/veins related to the mineralization in the Bayan Obo deposit, four types of REE mineralization are identified, including carbonatite dyke, ore-hosting dolomite marble, banded REE–Nb–Fe ore, and late-stage REE vein. Geochronology on these four types of mineralization, using U-Th-Pb, Sm-Nd, Rb-Sr, K-Ar, Ar-Ar, Re-Os, and La-Ba methods, has been reported in the last two decades. However, various dating methods gave different mineralization ages, resulting in long and heated debates. A compilation of age data for the Bayan Obo REE mineralization has a wide range, from >1800 Ma to ~390 Ma, with two peaks at ~1400 Ma and 440 Ma. The earliest ages, reported from zircons in the carbonatite dykes by SHRIMP or ID-TIMS with ages > 1800 Ma, are largely thought to be inherited zircons derived from the Palaeoproterozoic basement in the area. There are three main opinions on mineralization ages.

Mesoproterozoic mineralization: Nakai et al. (1989) first reported REE mineral La-Ba and Sm-Nd isochron date of 1350 ± 149 Ma and 1426 ± 40 Ma, respectively. In addition, Zhang et al. (2003) obtained mineral Sm-Nd isochron dates for ores at the Main and East Orebodies of 1286 ± 91 Ma and 1305 ± 78 Ma, respectively. We report here a whole-rock Sm-Nd isochron from of nine carbonatite dykes yielding a slightly older age of 1354 ± 59 Ma. Zircons collected from a carbonatite dyke were analyzed by conventional isotope dilution thermal ionization mass spectrometry (ID-TIMS),. The results arean upper intercept age of 1417 ± 19 Ma. This age is confirmed by SHRIMP U-Pb analysis of zircon from the same carbonatite dyke, which gave a $^{207}Pb/^{206}Pb$ weighted mean age of 1418 ± 29 Ma.

Early Paleozoic mineralization: Chao et al. (1997) made numerous Th-Pb dates for monazite and bastnäsite samples at Bayan Obo, and provided isochron ages for monazite mineralization ranging from 555 to 398 Ma. They proposed that intermittent REE mineralization of the Bayan Obo deposit started at about 555 Ma, and the principal mineralization occurred between 474 and 400 Ma. We used Sm-Nd dating of the REE mineral, huanghoite, and single-grain biotite Rb-Sr dating, showing concordant isochrons corresponding to 442 ± 42 Ma and 459 ± 41 Ma, respectively.

Two-stage mineralization: Campbell et al. (2014) reported SHRIMP dating of extremely U-depleted (<1 ppm) zircons from banded ores in the East Orebody. Their $^{232}Th–^{208}Pb$ geochronological data reveal the age of zircon cores with Mesoproterozoic ages as 1325 ± 60 Ma and a rim alteration event with Caledonian ages as 455.6 ± 28.27 Ma. Zhu et al. (2015) reviewed Sm–Nd isotopic measurements which were undertaken to constrain the chronology of REE mineralization events at Bayan Obo, and considered that a series of ages between ca. 1400 Ma and 400 Ma resulted from thermal disturbance and do not imply the existence of additional mineralization events. They proposed that the earliest REE mineralization event was at 1286 ± 27 Ma using a Sm–Nd isochron of coarse-grained dolomite and the carbonatite dikes in their vicinity, and a significant thermal event at ca. 400 Ma resulted in the formation of late-stage veins with coarse crystals of REE minerals

5 Nature of ore-forming fluids and sources

The study of the nature of ore-forming fluids at Bayan Obo is limited by the post depositional history of the ores, particularly in the earliest stages of the paragenesis like banded ores. Several possible sources of ore-forming fluids have been proposed for the Bayan Obo deposit, including deep source fluids, anorogenic magma, magmatic and metamorphic fluids, mantle fluids, and carbonatite magma/fluids. Which source of ore-forming fluids best favor REE mineralization is still disputed.

The available data on the oxygen, carbon, strontium and niobium isotope composition of the carbonatites, dolomites and obviously sedimentary limestones at Bayan Obo are taken to indicate that the large and coarse-grained dolomite was an igneous carbonatite, and that the finer grained dolomite recrystallized under the influence of mineralizing solutions which entrained groundwater. Sun et al. (2013) systematically investigated the Fe isotope compositions of different types of rocks from the Bayan Obo deposit and related geological formations, such as carbonatites, mafic dykes, and Mesoproterozoic sedimentary iron formation and carbonates. The Fe isotope fractionation between magnetite and dolomite, and between hematite and magnetite at Bayan Obo is small, indicating that they formed in very high temperature conditions. It is proposed that the Fe isotope systematics for the Bayan Obo deposit is consistent with those of magmatic products, but different from those of sedimentary or hydrothermal products reported previously. They concluded that the Bayan Obo ore deposit is of magmatic origin.

The nature of ore-forming fluids has been studied in fluid inclusions trapped in banded and vein ores at Bayan Obo (Fan et al., 2006). Three types of fluid inclusions have been recognized: two or three phase CO_2-rich, three phase hypersaline liquid-vapor-solid, and two phase aqueous liquid-rich inclusions. Microthermometry measurements indicate that the carbonic phase in CO_2-rich inclusions is nearly pure CO_2. Fluids involving in the REE-Nb-Fe mineralization at Bayan Obo might be REE-F-CO_2-NaCl-H_2O system. The coexistences of hypersaline brine inclusions and CO_2-rich inclusion with similar homogenization temperatures give evidence that immiscibility took place during REE mineralization. The original H_2O-CO_2-NaCl fluid with higher REE contents probably derived from a carbonatite magma. The presence of REE-carbonates as an abundant solid in inclusions in the ores shows that the original ore-forming fluids were very rich in REE, and therefore, laid a foundation to produce economic REE ores at Bayan Obo.

6 Possible ore genesis

The Bayan Obo deposit was likely associated in space and time with large-scale carbonatitic magmatic activity (ca. 1400 to 1300 Ma) in response to the long-term rifting and magma evolution in the north margin of North China

Craton. The depleted mantle model age (T_{DM}) from the Nd isotope data on carbonatite dyke and ore-hosting dolomite samples ranges from 1610 to 1790 Ma, and coincides with the initiation of the Bayan Obo rift (ca. 1750 Ma). Along with the prolonged and slow extension of the Bayan Obo rift, the mantle lithosphere underwent low degree of partial melting leading to the production of carbonatite magma at the final stage of break up of the Columbia supercontinent (ca. 1400-1200 Ma). Through continuous evolution (crystal fractionation), abundant LREE accumulation occurred in the terminal calcite carbonatite magma, which was then superposed on the early dolomite carbonatite pluton, thus resulting in the formation of the giant Bayan Obo REE deposit.

As the Bayan Obo ore deposit is LREE and Th enriched, U depleted, and has very low Sm/Nd and U/Pb values and low $^{206}Pb/^{204}Pb$ ratios, it is difficult to obtain high resolution Sm-Nd, U-Pb ages for banded and massive REE mineralization in the East and Main Orebodies. The zircons in the carbonatite dyke at Bayan Obo provide a unique record of the early mineralization history of the region. The timing of the early episode of REE mineralization of the Bayan Obo deposit obtained from REE minerals and ore-hosting dolomite, ca. 1400-1300 Ma, is consistent with the reported ages of REE-rich carbonatite dykes, implying a genetic connection. Geochemical evidence from element content and Nd isotope compositions also imply that ore-hosting dolomite and the carbonatite dykes have a close relationship to a magmatic origin. A significant thermal event at ca. 440 Ma resulted in the formation of late-stage veins with coarse crystals of REE minerals. However, the REE mineralization developed during this event resulted from remobilization of REE within the orebodies, and any potential contribution from external sources was minimal. Thus, this late mineralization event might make no significant contribution to the existing ore reserves. The ages of ca. 440 Ma may be related to subduction of the Palaeo-Asian oceanic plate during the Silurian.

It can be concluded that the Bayan Obo giant deposit is a product of mantle-derived carbonatitic magmatism at ca. 1400 Ma, which was likely related to the breakup of Columbia. Some remobilization of REE occurred due to subduction of the Palaeo-Asian plate during the Silurian, forming weak vein-like mineralization (Fig. 1).

Acknowledgements

Prof. Frances Wall is thanked for her constructive and valuable comments. This study is financially supported by the National Key Research and Development Program (Grant No. 2017YFC0602302).

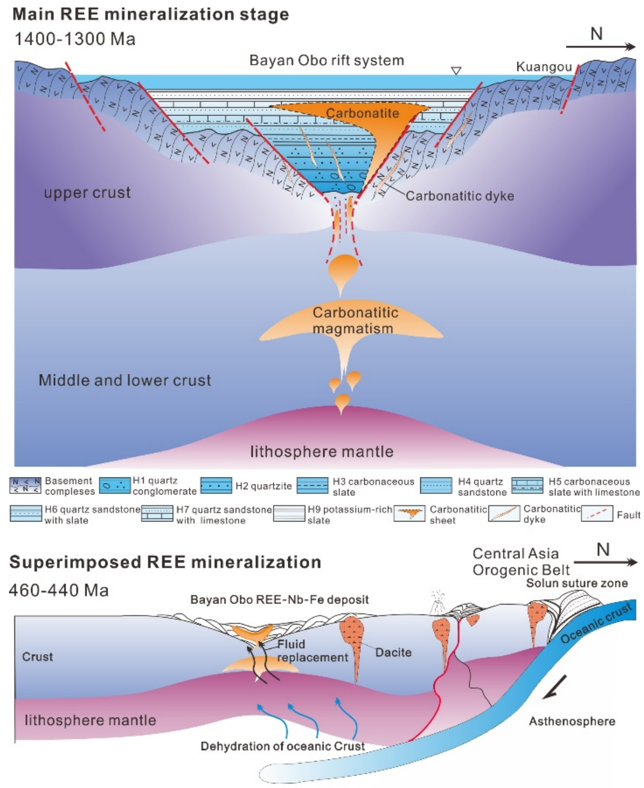

Figure 1. Two stage mineralization model for the formation of the giant Bayan Obo deposit

References

Campbell LS, Compston W, Sircombe KN, Wilkinson CC (2014) Zircon from the East Orebody of the Bayan Obo Fe–Nb–REE deposit, China, and SHRIMP ages for carbonatite-related magmatism and REE mineralization events. Contributions to Mineralogy and Petrology 168:1041

Chao ECT, Back JM, Minkin JA, Tatsumoto M, Wang J, Conrad JE, MaKee EH, Hou Z, Meng QS (1997). The sedimentary carbonate-hosted giant Bayan Obo REE-Fe-Nb ore deposit of Inner Mongolia, China: A cornerstone example for giant polymetallic ore deposits of hydrothermal original. US Geology Survey Bulletin 2143:1-65

Fan HR, Hu FF, Yang KF, Wang KY. (2006) Fluid unmixing/immiscibility as an ore-forming process in the giant REE-Nb-Fe deposit, Inner Mongolian, China: evidence from fluid inclusions. Journal of Geochemical Exploration 89:104–107

Nakai S, Masuda A, Shimizu H (1989) La-Ba dating and Nd and Sr isotope studies on Bayan Obo rare earth element ore deposit, Inner Mongolia, China. Economic Geology 84:2296-2299

Sun J, Zhu X, Chen Y, Fang N (2013) Iron isotopic constraints on the genesis of Bayan Obo ore deposit, Inner Mongolia, China. Precambrian Research 235:88–106

Yang KF, Fan HR, Santosh M, Hu FF, Wang KY. (2011) Mesoproterozoic carbonatitic magmatism in the Bayan Obo deposit, Inner Mongolia, North China: Constraints for the mechanism of super accumulation of rare earth elements. Ore Geology Reviews 40:122–131

Zhang ZQ, Yuan ZX, Tang SH, Bai G, Wang JH (2003) Age and Geochemistry of the Bayan Obo Ore Deposit. Geological Publishing House, Beijing, pp 1-222 (in Chinese with English Abstract)

Zhu XK, Sun J, Pan C (2015) Sm–Nd isotopic constraints on rare-earth mineralization in the Bayan Obo ore deposit, Inner Mongolia, China. Ore Geology Reviews 64: 543-553

Mechanisms for the generation of HREE mineralization in carbonatites: Evidence from Huanglongpu, China.

Martin Smith[1], Delia Cangelosi, Bruce Yardley[2], Jindrich Kynicky[3], Chen Xu[4], Wenlei Song[5], John Spratt[6]
[1]*School of Environment and Technology, University of Brighton, UK*
[2]*School of Earth and Environmental Sciences, University of Leeds, UK*
[3]*Mendel University in Brno, Brno, Czech Republic*
[4]*School of Earth & Space Sciences, Peking University, Beijing, China*
[5]*Department of Geology, Northwest University, Xi'an, China*
[6]*Natural History Museum, London, UK*

Abstract. The Hunaglongpu carbonatites, Qinling Mountains, China, are exceptional as they form both an economic Mo resource, and are enriched in the HREE compared to typical carbonatites, giving a metal profile that may closely match projected future demand. The carbonatites at the level currently exposed appear to be transitional between magmatic and hydrothermal processes. The multistage dykes and veins are cored by quartz which hosts a fluid inclusion assemblage with a high proportion of sulphate daughter or trapped minerals, and later stage, cross-cutting veins are rich in barite-celestine. The REE mineral paragenesis evolves from monazite, through apatite and bastnäsite to Ca-REE fluorcabonates, with an increase in HREE enrichment at every stage. Radio-isotope ratios are typical of enriched mantle sources and sulphur stable isotopes are consistent with magmatic S sources. However, Mg stable isotopes are consistent with a component of recycled subducted marine carbonate in the source region, The HREE enrichment is a function of both unusual mantle source for the primary magmas and REE mobility and concentration during post-magmatic modification in a sulphate-rich hydrothermal system. Aqueous sulphate is a none specific ligand for the REE, and this coupled with crystal fraction lead to HREE enrichment during subsolidus alteration.

Introduction

The rare earth elements have become a focus of intense economic interest because of the restriction in supply caused by a focus of production in China, coupled with increasing use in renewable energy and high technology applications. Rare earth element resources are dominated by concentrations associated with alkaline igneous rocks, notably carbonatites.

Element enrichments in carbonatite tend to be in the light REE (La to Nd). Middle to HREE enriched carbonatites do occur however, and may have REE distributions which are a closer match to project future REE demand than typical carbonatites (Goodenough et al., 2017). Here we present data on the geochemical and mineralogical evolution of the Huanglongpu carbonatites, China (Fig. 1), which show overall REE patterns that bridge a gap between typical and HREE mineralised carbonatites (Smith et al., 2018).

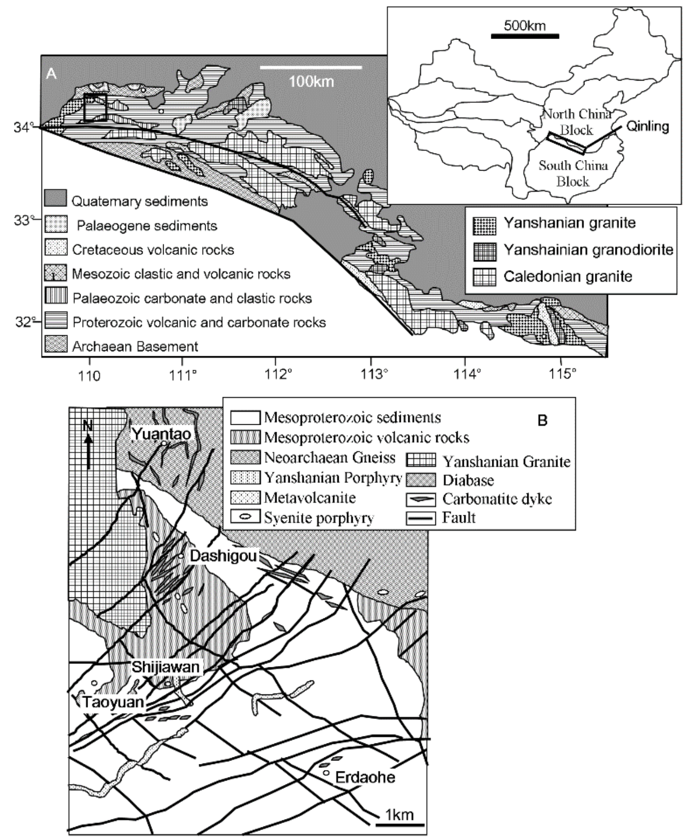

Figure 1: (A) Geological map of the eastern Qinling Mountains showing the location of the Huanglongpu area. Inset shows the overall location within China in relation to major crustal blocks.(B) Geological map of the Huanglongpu Mo-district (highlighted in bold in A). Maps adapted from Xu et al. (2010).

2 Geology

The Huanglongpu district is composed of four carbonatite-related orefields (Fig. 1) with a total ore reserve of N180 Kt of Mo. Re-Os dates indicate the dykes are 50-90Ma older than porphyry mineralisation in the district and hence not related to overprinting sulphide mineralisation (Song et al., 2016; Stein et al., 1997). The ore bodies occur discontinuously over a total distance of 6 km and an area of 23 km^2.

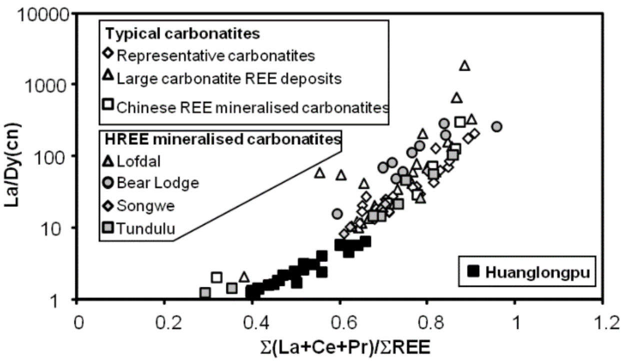

Figure 2: Comparison of ratios characterising the REE pattern for the Huanglongpu carbonatites with typical carbonatites (diagram and references from Smith et al., 2018).

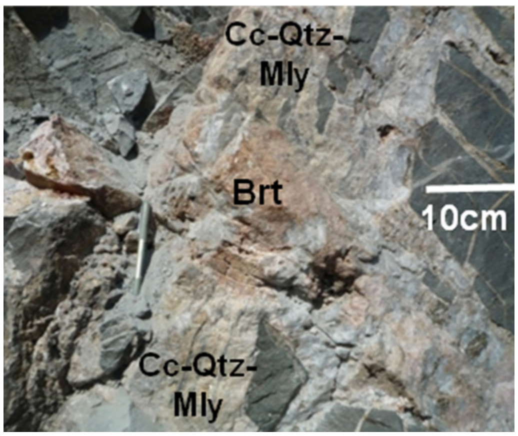

Figure 3: Example of field relationships in the Huanglongpu carbonatites, with a calcite-quartz-molybdenite dyke cross-cut by a conjugate barite-rich dyke (Smith et al., 2018)

The carbonatite dykes are highly parallel, predominantly dipping N to NNW, at steep angles (strike/dip ~260/50–88°N) and consist of calcite, kutnahorite, quartz, potassium feldspar, barite, pyrite, galena, sphalerite, molybdenite, monazite, Ca-REE-fluorcarbonates, apatite, britholite, pyrochlore, uraninite, REE fluorides, burbankite, celestine, strontianite and brannerite. Minor fluorite is found at Shijiawan and Yuantao. The dykes range in thickness from ~10m to ~0.1m (Fig. 3) with lateral extents ranging from 10m to N1 km. Rarer dykes occur in orientations conjugate to the main set (strike/dip ~350/50–80°E). Minor offsets suggest this set may be slightly later than the main set, although the conjugate orientation and presence of conjugate veins merging with the main set suggest they were very nearly contemporaneous. Barite-celestine bearing dykes and veins cut the earlier carbonate-quartz-sulphide bearing dykes (Fig. 3). Quartz is dominantly restricted to cores of dykes and may be mainly hydrothermal in origin. This suggests the primary dykes may have been calico-carbonatite in composition although the bulk dyke composition is silico-carbonatite. In the carbonatites, molybdenite occurs mainly as disseminated grains and intergranular and fracture-hosted films, sometimes associated with pyrite, galena and sphalerite suggesting a subsolidus, hydrothermal origin for at least some of the sulphide assemblage. Disseminated molybdenite is also found along fractures in fenitized gneiss near its contact with the dykes. The overall HREE enrichment of the Huanglongpu carbonatites has been previously related to a recycled ocean crust component in the lithospheric mantle indicated by Nd-Sr radioisotope studies and Mg stable isotope analyses of calcite (Song et al., 2016). This primary source control has been proposed to be enhanced by fractional crystallisation of calcite, with the dykes at the current level of exposure representing relatively HREE-enriched carbonate residuum (Xu et al., 2007).

3 Results

3.1 REE mineral paragenesis

The earliest stage of REE mineralization is the formation of monazite-(Ce) as eu- to subhedral crystals within calico carbonatite. Monazite is a potentially magmatic phase as it is fractured, and the fractures subsequently filled by the sulphide mineral assemblage, specifically molybdenite. Additional potentially early REE-bearing phases include pyrochlore, apatite, zircon and parisite which occurs intergrown with galena and molybdenite. Monazite is overgrown and replaced by apatite, which is in turn overgrown and replaced by britholite-(Ce) ($REE_3Ca_2SiO_4F$) (Fig. 4). The formation of britholite is accompanied by the formation of allanite-(Ce) in the surrounding rock. Both are common in the quart-rich cores to the dykes. Within the fluorcarbonate assemblage early bastnäsite-(Ce) and parisite-(Ce) are replaced by parisite-synchysite-(Ce) syntaxial intergrowths, and by röntgenite-(Ce). At the same time as the development of the REE mineral paragenesis the early niobium phases undergo alteration. Early aeschynite-(Ce) is altered to urano-pyrochlore, which is then altered to pyrochlore with uraninite inclusions.

3.2 Mineral chemistry

Analyses of REE and niobate mineral chemistry where carried out by EMPA and LA-ICPMS at the Natura History Museum, London. Figure 5 shows typical chondrite normalized REE patterns for phosphates and flurocarbonates. In all cases the mineral chemistry is dominated by the LREE, and all REE minerals are the Ce-dominant variety. However, there is a clear distinction in HREE contents between monazite and apatite and britholite, with the latter being significantly more HREE-rich. The same is also true of the fluorcarbonates, and aeschynite, urano-pyrochlore and pyrochlore, with the level of HREE enrichment increasing in later paragenetic stages (Fig. 5). When minerals are normalized to their precursor phase identified from textural studies, it becomes apparent that at every stage of alteration the REE minerals become more HREE-rich (Fig. 6).

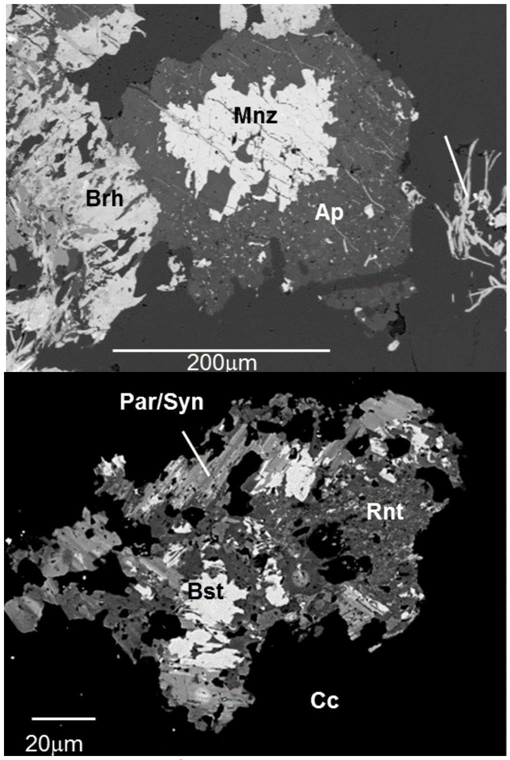

Figure 4: Examples of mineral textures at Huanglongpu as backscattered electron images. (A) Monazite replaced by apatite, which is in turn replaced and overgrown by britholite. (B) Bastnäsite overgrown by syntaxially intergrown pariste and synchysite, followed by röntgenite. (Smith et al., 2018).

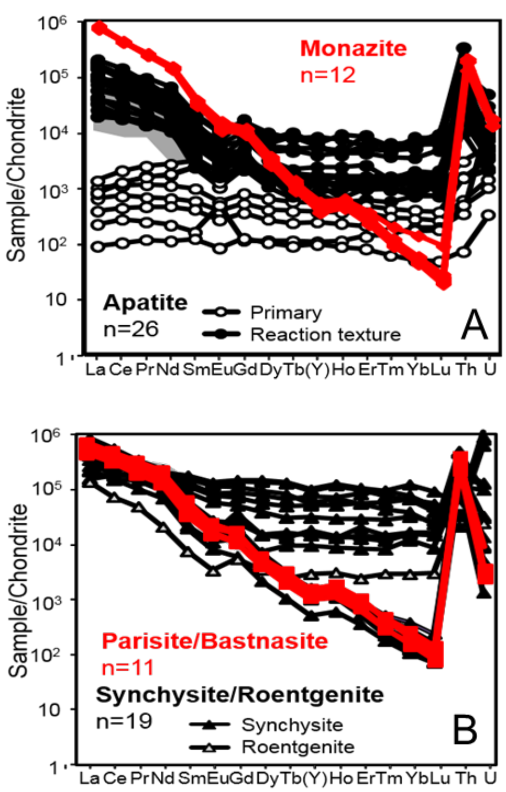

Figure 5: Chondrite normalized REE patterns for phosphates and fluorcarbonates from Huanglongpu. Determined by LA-ICPMS. Th and U are included to illustrate actinide behavior (Smith et al., 2018).

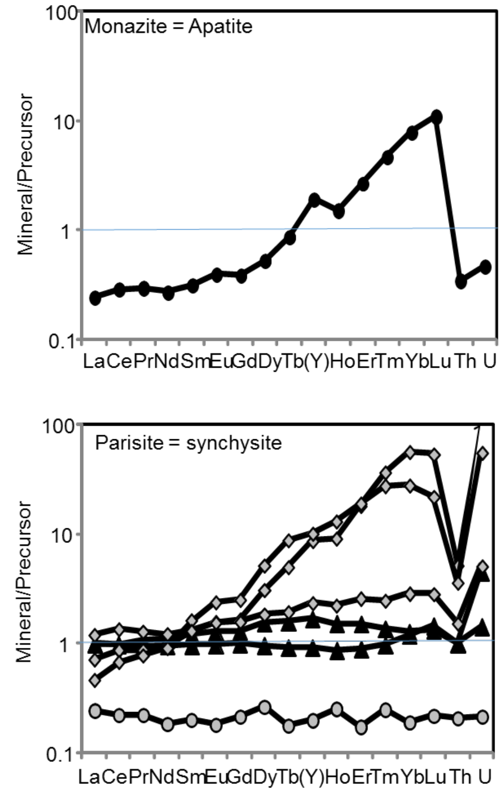

Figure 6: Composition of minerals in reaction textures normalised to the precursor phase for phosphates and fluorcarbonates (Smith et al., 2018).

3.3 Fluid evolution

Fluid inclusions in quartz have been studied by Song et al, (2016) and as part of this study. Early aqueous-carbonic fluid inclusions containing sulphate minerals contain nearly pure CO_2, and have salinities in the aqueous phase determined from clathrate melting of 5–19 wt% NaCl equivalent, although high SO_4 contents may mean these estimates are significantly in error. These inclusion decrepitate on heating, and so homogenisation temperatures cannot be determined. They occur in assemblages with liquid CO_2 inclusions. Laser Raman spectroscopic data from inclusions in quartz cores to the carbonatite dykes indicate arcanite (K_2SO_4), anhydrite ($CaSO_4$), glauberite ($Na_2Ca(SO_4)_2$), aphthitalite ($(K,Na)_3Na(SO_4)_2$ and gorgeyite ($K_2Ca_5(SO_4)_6 \cdot H_2O$) within fluid inclusions (Fig. 7). The wide range in solids suggests heterogeneous trapping following sulphate saturation triggered by mixing with a CO_2-rich fluid, or with CO2 generated by reactions of the acid sulphate fluid with carbonatite calcite Fluid inclusions in fracture-fill quartz and calcite are typically 2 phase aqueous liquid plus vapour inclusions. These homogenise between 265 and 120 °C, and have salinities from 6 to 15wt% NaCl eq. Early quartz and calcite from Huanglongpu analysed by SIMS mostly give $\delta^{18}O$ values close to 10 ‰. The very small fractionation between the two minerals is indicative of near-magmatic temperatures. Thin crack-fills of secondary quartz, identified by CL imaging, are of very similar composition to the primary quartz, but a secondary crack-fill calcite is around 3 ‰ heavier, which may indicate a temperature below 200ºC if both crack-fills equilibrated.

Overall these data suggest that initial REE mineralisation took place at late magmatic temperatures. Early fluid inclusions were heterogeneously trapped from sulphate saturated brines which either mixed with CO_2-rich fluids, or generated CO_2 via water-rock interaction between 300 and 200 °C and 100-50 MPa. Late hydrothermal quartz deposition and the alteration of REE minerals took place down to 120°C, at pressures below 100 MPa. These fluids where present throughout REE mineral deposition.

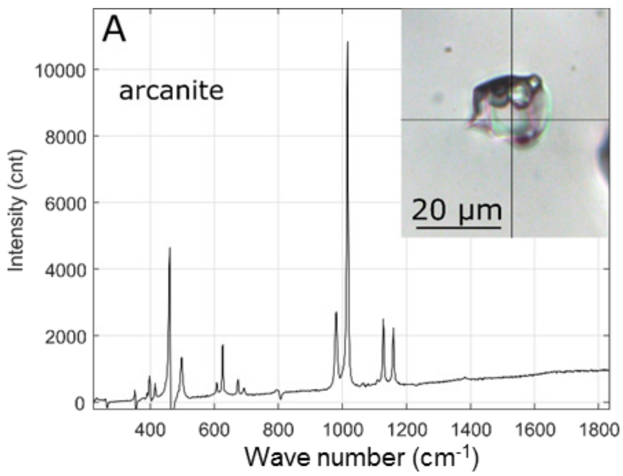

Figure 7: Example of a laser Raman spectrum of fluid inclusion hosted minerals in quartz hosted fluid inclusions from Huanglongpu. In this case the solid phase is identified as arcanite (K_2SO_4).

4 Discussion and conclusions.

Previous studies have demonstrated that the relative HREE enrichment of the Huanglongpu carbonatites relates to the primary magmatic source, with potential inputs from sedimentary carbonate recycled into the mantle via subduction (Song et al., 2016), followed by fractional crystallisation of LREE-rich phases resulting in further HREE enrichment of the residual carbonatite magma (Xu et al., 2007). This initial enrichment has been enhanced at the current level of exposure by hydrothermal processes involving sulphate-rich brines from sub-solidus temperatures down to ~120°C.

The REE mineral paragenesis evolved throughout this process. Monazite and possibly some LREE-rich fluorcarbonates formed as magmatic phases. Subsequent depletion of the residual magma in the REE, coupled with increasing Ca-activity resulted in the reaction of monazite to apatite. The onset of hydrothermal conditions, marked by the quartz cores to the dykes, caused the reaction of apatite with REE-bearing hydrothermal fluids to form britholite. Continuous cooling and dilution of this system resulted in calcite dissolution and the formation of progressively more Ca-rich REE fluorcarbonates.

The presence of sulphate as the dominant ligand in the hydrothermal fluid resulted in preferential transport and deposition of the HREE during mineral alteration. Experimental studies have shown that most common ligands (in particular Cl^-) promote preferential solubility of the LREE (Migdisov et al., 2009; Tropper et al., 2011). However, SO_4^{2-} shows no preferential complex ion formation with the REE, and may therefore have leached the REE from HREE enriched calcite without significant fractionation (Migdisov and Williams-Jones, 2008). Sulphate enrichment in carbonatites may therefore be important in the development of HREE-rich mineral assemblages, alongside specialised magmatic source regions.

Acknowledgements

This work was supported by the NERC SOS:RARE project (NE/M011267/1) and NERC Ion Microprobe facility grant IMF639/1017.

References

Goodenough KM, Wall F, Merriman D. (2018) The Rare Earth Elements: Demand, Global Resources, and Challenges for Resourcing Future Generations. Nat Resour Res 27:201-216.

Migdisov A.A., Williams-Jones A.E., Wagner T. 2009. An experimental study of the solubility and speciation of the Rare Earth Elements (III) in fluoride- and chloride-bearing aqueous solutions at temperatures up to 300°C. Geochimica et Cosmochimica Acta 73, 7087–7109.

Migdisov A.A., Williams-Jones A.E. 2008. A spectrophotometric study of Nd(III), Sm(III) and Er(III) complexation in sulfate-bearing solutions at elevated temperatures. Geochimica et Cosmochimica Acta 72, 5291–5303.

Song, W., Xu, C., Smith, M.P., Kynicky, J., Huang, K., Wei, C., Li Zhou, Shu, Q. 2016. Origin of unusual HREE-Mo-rich carbonatites in the Qinling orogen, China. Scientific Reports 6:37377 | DOI: 10.1038/srep37377.

Smith M, Kynicky J, Xu C et al (2018) The origin of secondary heavy rare earth element enrichment in carbonatites: Constraints from the evolution of the Huanglongpu district, China. Lithos 308-309:65-82.

Stein, H.J., Markey, R.J.,Morgan, M.J., Du, A., Sun, Y., 1997. Highly precise and accurate Re–Os ages for molybdenite from the East Qinling–Dabie molybdenum belt, Shaanxi province, China. Economic Geology 92, 827–835.

Tropper, P., Manning, C.E., Harlov, D.E. 2011. Solubility of $CePO_4$ monazite and YPO_4 xenotime in H_2O and H_2O–NaCl at 800 °C and 1 GPa: Implications for REE and Y transport during high-grade metamorphism. Chemical Geology 282, 58–66

Xu, C., Campbell, I.H., Allen, C.M., Huang, Z.L., Qi, L., Zhang, H., Zhang, G.S. 2007. Flat rare earth element patterns as an indicator of cumulate processes in the Lesser Qinling carbonatites, China. Lithos 95, 267–278.

Diversity of ores in carbonatite-related rare earth deposits

Liu Yan
Institute of Geology, Chinese Academy of Geological Sciences, Beijing, PR China.

Abstract. Carbonatite-related REE deposits have various ore type characteristics, including the scales and ore-formation structures. The Cenozoic Mianning–Dechang (MD) rare earth element (REE) belt in eastern Tibet has several carbonatite-related REE deposits, with large and medium scales and a series of ore types such as brecciated, weathered and disseminated. According to petrographic studies, REE mineralization occurred with large scale overprinted gangue minerals such as barite, fluorite, calcite formed at the last hydrothermal stage and all these REE ores formed within an limited ranges of temperature and pressure. According to new detailed geological mapping, the variety of different ore types are a result of local tectonic structure rather than different depths. For instance, brecciated and weathered ores in the Dalucao deposit were controlled by frequent brecciation and fracture activities around the deposit. Ore veins controlled by tensional fissures arose by the same Haha fractures in Maoniuping deposit. As a result of fewer tectonic activities, disseminated ores only are found only in Lizhuang deposit. Thus, these various types of ores were controlled by different tectonic structures. Despite the various ores types, REE originate directly from the carbonatite-syenite complex. The ore variety is mainly caused by the different ore-controlling structures.

1 Introduction

The genesis of carbonatite-related REE deposits is not a simple one-stage process of ore deposition. Because of this complexity and the variety of ores, deciphering the evolution of these deposits is a challenging task that requires a meticulous study of petrography, geochemical characteristics of ores, tectonic activities, and variations in the distribution and composition of their constituent minerals. The Cenozoic Mianning-Dechang (MD) belt (Liu et al., 2015a) offers excellent opportunities for studying the genesis of variety of carbonatite-related REE ores.

The MD belt (Fig. 1) is situated in eastern Tibet and western Sichuan (southwestern China), and measures about 270 km in length and 15 km in width (Fig. 2). The MD belt contains REE deposits that all formed under the same geological conditions, but these deposits have various grades, reserves, and REE mineralization styles. As such, study of these deposits with regards to REE mineralization may further our understanding of the formation of large carbonatite-associated REE deposits (CARDs).

Schematic illustrations of models for CARD formation have been set up by Hou et al. (2015) including a variety of carbonatite-related deposits. This model includes a variety of orebodies formed by fluids exsolved from REE-rich carbonatitic magmas emplaced at shallow crystal levels. Lateral migration, replacement, open-space filling, and focused discharges of ore-forming fluids produced semi-stratabound (Bayan obo-style), disseminated (Lizhuang or Mountain Pass-style), stringer-stockwork (Moniuping -style) and breccia pipe (Dalucao-style) orebodies, with associated fenitization and K-silicate alterations, respectively (Hou et al. 2009). This model has been obtained from the depth of the ores, ore-controlling structures and appearance of carbonatite-related ores, but comparison of these deposits in terms of the formation of various types and scales of ores are still unclear.

Herein, based on literature studies and this work, the origin (carbonatite-syenite complex), formation stages, evolution and composition of ore-forming fluids and the local structural controls on the shape of orebodies have been systematically compared.

2 Geology of REE deposits in the Mianning-Dechang Belt

The MD Belt, which is in western Sichuan Province, southwest China, is ~270 km long and 15 km wide (Fig. 1). The NS-trending belt of carbonatite-nordmarkite complexes (Fig.2), bounded by the Yalongjiang and Anninghe strike-slip faults, intrudes the Proterozoic crystalline basement rocks and Paleozoic-Mesozoic sedimentary sequences. In individual complex, carbonatites occur as sills, dykes, stocks, and hypabyssal intrusions within the nordmarkite intrusions. The belt hosts the Maoniuping, Muluozhai, Lizhuang, and Dalucao REE deposits (Fig. 2) and contains a total estimated resource of over 3 Mt of light rare earth oxides (REO) (Hou et al., 2009).

The location of the Maoniuping nordmarkite-carbonatite pluton is controlled by the Haha strike-slip fault, which is a secondary structure with respect to the MD fault. Most carbonatite bodies (referred to as “sills” in previous publications) are in the northern part of the intrusion (Guangtoushan section). Although the currently mined part of the deposit (Dagudao section) contains some carbonatite bodies, their proportion is relatively small. This section consists predominantly of quartz nordmarkite, which hosts a stockwork grading into multiple branching veins of variable thickness. Fenitization, manifested by mica-, sodium clinopyroxene- and amphibole-rich zones, is very prominent at Dagudao, where it is spatially associated with REE mineralization.

In contrast to the other deposits in the MD belt, the REE ores at Maoniuping are hosted by a structurally complex system of mineralized veins, veinlets and stockwork zones, which has an “S”-like outline in plan view and extends roughly in a NNE-SSW direction (Fig. 2A). This configuration suggests that the mineralization was controlled by strike-slip faulting. Geological cross-sections along a series of exploration lines, constructed on the basis of drill-core data, suggest that the Dagudao section is the core area of the Maoniuping deposit (Yuan et al. 1995).

Thick veins are particularly common in the southeastern part of the Dagudao section, i.e. down-slip from the core area. Breccias are composed of angular wall-rock nordmarkite clasts set in a matrix of ferromagnesian silicates (predominantly, sodium clinopyroxene and amphibole). Locally, pervasively fenitized older metamorphic rocks are also present as clasts.

The Muluozhai REE deposit is divided into the Diaoloushan and Zhengjialiangzi areas, which contain six main orebodies. The deposit is in the northern segment of the MD Belt and is controlled by the strike-slip Yalongjiang Fault, which connects with the Xianshuihe Fault to the north. The Permian units are part of a thick sequence of Permian–Triassic marble and basalt with minor sandstone and other clastic sediments. The REE-mineralization is hosted in veins and veinlets along the fractured contact between metadiabase and nordmarkite or marble.

The Lizhuang carbonatite–nordmarkite complex intrudes metamorphosed Silurian–Triassic clastic and carbonate rocks (Fig. 2C). The complex is 100–150 m wide, 400 m long, and consists of NNW–SSE-striking carbonatite sills and a nordmarkite pluton. The main REE orebody is elongate parallel to the contact zone between the carbonatite–nordmarkite complex and the surrounding wall rocks. The principal ore mineral is bastnäsite, which formed synchronous with the alteration of the carbonatite–nordmarkite complex (Fig. 3E). In contrast to the other deposits in the MD Belt, ore mineralization could be found in nordmarkite and carbonatite in the Lizhuang deposit respectively (Fig. 3F).

The Lizhuang deposit comprises massive fluorite–quartz–calcite–bastnäsite ores and minor brecciated ores. The individual orebodies are 30–100 m long and 2.2–11.6 m thick (Fig. 2C). There are four types of ore; yellow-banded, stockwork, black brecciated, and the principal brown-colored disseminated ore.

The Dalucao deposit is the only deposit in the southern part of the MD belt, and contains three orebodies (No. 1, No. 2, and No. 3; Fig. 2D). No. 1 and No. 3 orebodies are hosted in breccia pipes within carbonatite–nordmarkite host rocks, and have similar grades, at 1.0–4.5 % REO. Both pipes are elliptical in plan-view, with long-axes of 200–400 m and short-axes of 180–200 m. The pipes extend downwards for >450 m. The REE mineralization was controlled by the Dalucao Fault. Faulting and brecciation facilitated the circulation of ore-forming fluids and provided space for REE precipitation.

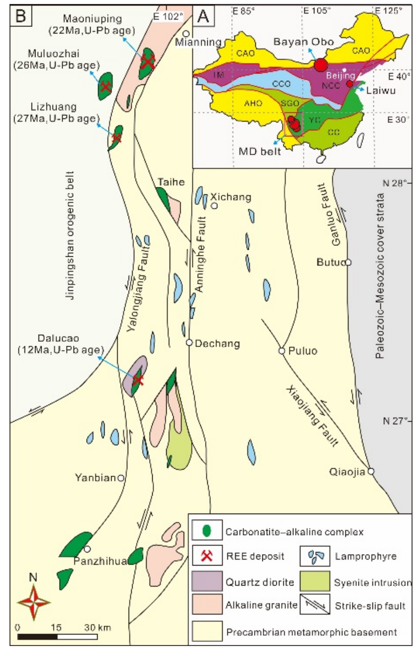

Figure 1. Location, geology, and tectonics of the Maoniuping, Muluozhai, Lizhuang, and Daulcao REE deposits. A) Overview map of the tectonic regions of China. NCC - North China Craton, TM - Tarim Block, YC - Yangtze Craton, CC - Cathaysia Craton, CAO - Central Asia Orogeny, CCO - Central China Orogeny, AHO - Alps-Himalaya Orogeny, SGO - Songpan-Ganze orogeny. B) Geological map showing the distribution of Cenozoic carbonatite–alkaline complexes in western Sichuan and the locations of reactivated faults and illustrating clearly that the faults cut the nordmarkite and carbonatite bodies. (modified from Yuan et al., 1995).

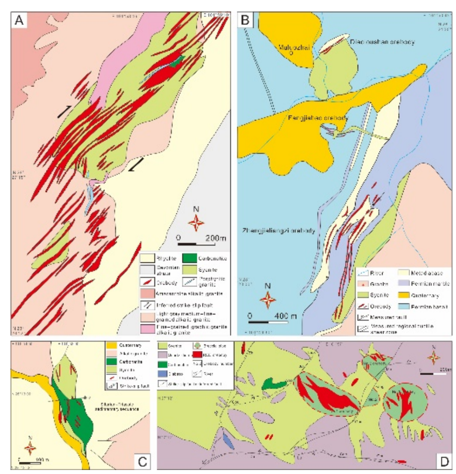

Figure 2. (A) Simplified geological map showing the distribution of carbonatite–alkaline complexes and associated REE orebodies within the Maoniuping deposit (modified from 109 Geological Brigade of Sichuan Bureau of Geology and Mineral Resource, 2010). (B) Geological map of the Muluozhai ore district (Institute of Multipurpose Utilization of Mineral Resources, Chinese Academy of Geological Sciences, 2008). (C) Schematic geological map showing the key features of the nordmarkite–carbonatite complex and associated REE orebodies within the Lizhuang deposit (modified from Hou et al., 2009). (D) Geological map showing the key features of the nordmarkite–carbonatite complex and associated REE orebodies within the Dalucao deposit (modified from Yang et al., 1998).

Despite multiple phases of brecciation (four events are recorded in each of the pipes), mineralized veins and ores are contained wholly within altered nordmarkite at Dalucao (Liu et al., 2015b). The ores are weathered, brecciated, and dominated by fine-grained REE minerals (Fig. 3D) (Liu et al., 2015b, c). Brecciated ores are the main ore type, and it is notable that coarse-grained REE minerals are rare in the Dalucao deposit. Clasts within the breccia pipes are dominantly of magmatic origin, or are composed of carbonate minerals. Pyrite, fluorite, barite, celestine, muscovite, quartz, and REE minerals all occur throughout the matrix. In the No. 3 orebody, REE-mineral-bearing hydrothermal carbonate veins crosscut the other breccias, and represent another type of breccia ore.

3 Alteration and formation stages

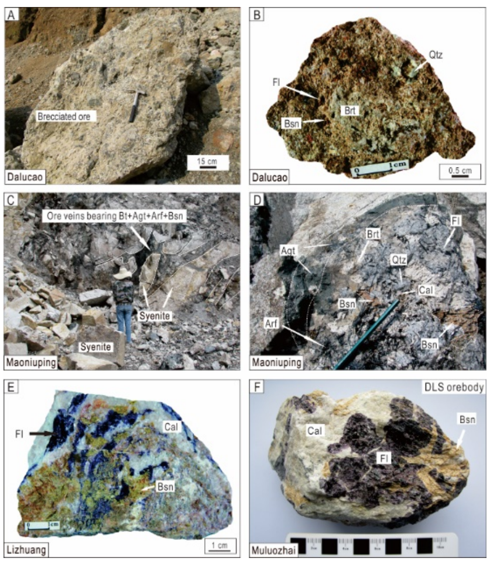

Figure 3. Macroscopic features of bastnäsite from the MD REE belt. (A) Brecciated ore in orebody No. 3 of the Dalucao deposit. (B) Weathered ore containing fluorite, quartz, barite, and bastnäsite in orebody No. 1 of the Dalucao deposit. (C) Ore veins containing a bastnäsite –aegirine–augite–arfvedsonite–biotite assemblage in syenite at Dagudao, Maoniuping deposit. (D) Mineral zoning from aegirine–augite, arfvedsonite, fluorite, calcite, barite, quartz, to bastnäsite within fractures in syenite. (E) Disseminated ore containing bastnäsite overprinting fluorite and calcite. (F) Typical massive ores containing fluorite, calcite, pyrite, and bastnäsite , Diaoloushan orebody, Muluozhai deposit. Mineral abbreviations are as follows: Brt (barite), Bsn (bastnäsite), Bt (biotite), Cal (calcite), Cls (celestite), Fl (fluorite), Gp(gypsum), Py(pyrite) and Qtz (quartz). From Guo and Liu (2019).

Alteration to biotite is the main alteration of syenite by hydrothermal fluids in these REE deposits. Gangue minerals such as fluorite, quartz, calcite and barite formed and overlapped with the biotite formation. In contrast, in the Maoniuping deposit, strong alteration of syenite by biotite-aegirine-augite-arfvedsonite was found. This is rare among these four deposits and may explain the formation of such a large REE deposit. In the Dagudao REE orebody at Maoniuping. The mineralized veins are invariably zoned; from the contact inwards, biotite- and K-feldspar-rich selvages are followed by zones dominated by aegirine-augite and arfvedsonite, and a core composed predominantly of barite, fluorite, calcite, and bastnäsite.

Among the REE belt, various types of ores can be found such as weathered ore, brecciated ore, ore veinlet or veins. According to the mineral assemblages, bastnäsite is the predominant REE mineral with lesser amounts of monazite and others. Also, in these ores, the bastnäsite always formed at the later stages during the evolution of hydorthemal fluids.

Generally, magmatic, pegmatitic and hydrothermal stages are main stages for the whole process for the formation of carbonatite-related REE deposits. Among these deposits, it is the large deposits such as Dalucao and Maoniuping deposits rather than the small deposits that have pegmatitic stages.

4 Typical stable mineral assemblages in various types of ores in MD REE belt

According to the scale, stages, mineral assemblages and their characteristics in individual stages, a comparative summary of these four deposits could be obtained. Generally, the stable mineral assemblage containing fluorite, barite, calcite and bastnäsite occurs in a late hydrothermal stage in the various ore types. As fluid inclusions in bastnäsite crystals have low homogenization temperatures below 350℃ and pressures of 2.0–2.4 kbar. (Zheng and Liu, 2019), large scale bastnäsite mineralization is only found during the late stage of hydrothermal fluid evolution. Actually, typical ores along Mianning-Dechang REE belt commonly include fluorite, barite, calcite and bastnäsite. Without fluorite, REE ores commonly have low grades below 2%. Among this mineral assemblage bearing bastnäsite, Ca, Ba, Sr, REE and F, SO_4^{2-}, CO_2 are closely related to each other, implying they are important for REE transport and precipitation. Also, in recent studies, Cl- is also regarded as the important ion for the transport of REE (Liu et al., 2018).

5 Sources of REE metals

Although the Dalucao, Maoniuping, Lizhuang, and Muluozhai REE deposits have various ore types and styles of mineralization, they are all hosted by similar carbonatite–syenite complexes.

According to the four stages after the emplacement of carbonatite-syenite complex, bastnäsite formed at the latest stage after the magmatic stage, pegmatite stage and hydrothermal stage. Petrographic investigations suggest that the bastnäsite within these deposits formed after the precipitation of fluorite, celestine, and barite minerals (Liu and Hou, 2017).

Except bastnäsite has high content of REE, minerals such as barite, celestine, and fluorite from both pegmatite and hydrothermal stages along the MD belt have the similar REE patterns and trace elements compositions with those of carbonatite-syenite complex. Also, all these minerals from various stages and carbonatite, syenite have similar Sr–Nd–Pb isotopic compositions to the hosting carbonatites and syenites, suggesting that the carbonatites, syenites, and REE mineralization are intimately related in origin.

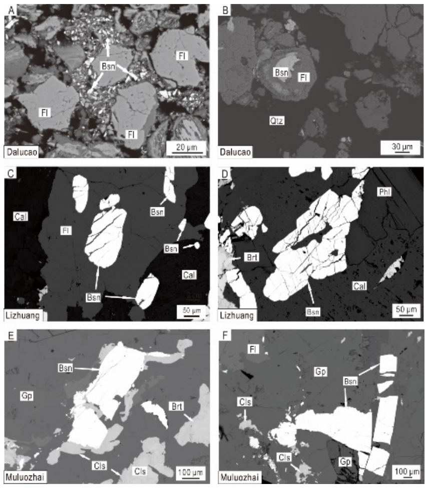

Figure 4.BSE images of REE ores in the MD belt. (A) bastnäsite in breccias overprinting fluorite in orebody No. 3, Dalucao deposit. (B) Weathered ore in orebody No. 1, Dalucao deposit. (C) and (D) Disseminated ore containing bastnäsite overprinting fluorite, calcite, and barite from the Lizhuang dposit. (E) and (F) Typical massive ores from the Diaoloushan and Zhengjialiangzi orebodies of the Muluozhai deposit, respectively, showing bastnäsite overprinting celestite, gypsum, and fluorite. Collectively, these images show that the REE mineralization overprinted earlier gangue minerals and therefore developed during the later stage of the hydrothermal evolution. From Guo and Liu (2019).

6 Local structure controlling orebody

Due to the scales and different types of faults and the distance between REE deposits, the effects on carbonatite-syenite complex and their wallrocks are quite different. For example, in the Maoniuping and Dalucao deposits, strong and frequent effects by faults led to the large amount of ore veins in Guangtoushan orebody in Maoniuping deposit and both brecciated and weathered ores in Dalucao deposit. But for Lizhuang REE deposit, with less effect from tectonic activities, only disseminated ores were found. In previous studies, it is assumed that REE could not be transported easily. But in the Maoniuping and Zhengjialiangzi deposits, wallrock such as alkali granite and marble, also hosts veinlet or veins. In fact, most of the ore occurs in the marble. In general, REE have been transported for relatively long distances into various types of wallrock.

Various types of ores point to one result that REE ores could be found in various types of fissures. Only in these fissures, pressures and temperatures could drop dramatically with infiltration of meteoric water. Then, REE mineralization mainly occurred under the similar conditions.

7 Conclusions

Despite various types of ores, REE mineralization occurs under a limited ranges of temperatures and pressures. Thus, the depth of the ores is not the main control on the various types of ores. Despite the different ore types, mineral assemblages of fluorite, calcite, barite and bastnäsite are stable in the higher grade ores rather than barite and bastnäsite and other mineral assemblages (<2%). This mineral assemblage reflects the effective transport and precipitation of REE during the evolution of hydrothermal fluids as F, SO_4, Cl and CO_3 and REE could form complexes that are destroyed under lower temperature and pressure. According to the geological setting and observation, local tectonic setting controls the ore formation. Brecciation and fissures caused the brecciated ore, ore veins and veinlets. The disseminated ore formed under less active tectonic conditions.

Acknowledgements

The study was funded by the Natural Sciences Foundation of China (grant no. 41772044).

References

Guo D X, Liu Y, 2019. Occurrence and geochemistry of bastnäsite in carbonatite-related REE deposits, Mianning-Dechang REE belt, Sichuan Province, SW China, Ore Geol Rev 107:266–28

Hou ZQ, Tian SH, Xie YL, Yang ZS, Yuan ZX, Yin SP, Yi LS, Fei HC,Zou TR, Bai G, Li XY (2009) The Himalayan Mianning-Dechang REE belt associated with carbonatite-alkaline complexes, eastern Indo-Asian collision zone, SW China. Ore Geol Rev 36:65–89

Hou ZQ, Liu Y, Tian SH, Yang ZM, Xie YL (2015) Formation of carbonatite-related giant rare-earth-element deposits by the recycling of marine sediments. Sci Rep 5:10231

Liu Y, Hou ZQ (2017) A synthesis of mineralization styles with an integrated genetic model of carbonatite-syenite-hosted REE deposits in the Cenozoic Mianning-Dechang REE metallogenic belt, the eastern Tibetan Plateau, southwestern China. J Asian Earth Sci 137:35–79

Liu Y, Chen ZY, Yang ZS, Sun X, Zhu ZM, Zhang QC (2015a) Mineralogical and geochemical studies of brecciated ores in the Dalucao REE deposit, Sichuan Province, southwestern China. Ore Geol Rev 70:613–636.

Liu Y, Zhu ZM, Chen C, Zhang SP, Sun X, Yang ZS, Liang W (2015b) Geochemical and mineralogical characteristics of weathered ore in the Dalucao REE deposit, Mianning-Dechang REE Belt, western Sichuan Province, southwestern China. Ore Geol Rev 71:437–456

Yuan ZX, Shi ZM, Bai G, Wu CY, Chi RA, Li XY (1995) The Maoniuping rare earth ore deposit, Mianning County, Sichuan Province. Seismological Publishing House, Beijing, p 150 (in Chinese

Zheng X, Liu Y, 2019. Mechanisms of element precipitation in carbonatite-related rare-earth element deposits: evidence from fluid inclusions in the Maoniuping deposit, Sichuan Province, southwestern China. Ore Geol Rev 107, 218-238

Deposit or prospect? example from the Miaoya, Hubei province, China

Dexian Zhang
Key Laboratory of Metallogenic Prediction of Nonferrous Metals and Geological Environment Monitor (Central South University), Ministry of Education, Changsha, China
School of Geosciences & Info-physics, Central South University, China

Yan Liu
Key Laboratory of Deep-Earth Dynamics, Institute of Geology, Chinese Academy of Geological Sciences, China

Abstract. The Miaoya carbonatite–syenite complex is prospective for REE and is ideal for studies of the formation of REE deposits. Mineralization at this prospect includes carbonatite-, syenite-, and mixed-type, all are low REE grade (below 1 %).

XRD and EMPA analyses reveal that REE minerals are low in all samples (<5%), consistent with the fact that few monazite, bastnäsite and other REE minerals are visible under the microscope. LA–ICP–MS analyses reveal that apatite and calcite in carbonatite have the highest REE concentrations. Isotope ratios of Sr and Nd for REE-mineralized and altered carbonatite and syenite rocks are similar to those of fresh carbonatites and syenites. These observations are interpreted as recording REE mineralization that originates directly from the unmineralized carbonatite–syenite complex rather than other host rocks. Carbon and oxygen isotope ratios of hydrothermal calcite are consistent with low-temperature alteration subsequent to ore formation.

The low REE of the Miaoya prospect compared with other carbonatite-syenite hosted deposits may reflect: 1) as supported by petrography, minimal tectonic deformation in the area resulting in 2) restricted cycling of hydrothermal solutions that led to 3) minimal fluid scavenging from REE-rich apatite and calcite for local REE re-deposition and concentration.

1 Introduction

China is known for its wide range of REE deposits, which have been producing since the 1980s. The genesis of China's giant carbonatite-hosted REE deposits involved a sequence of tectonic, magmatic, and hydrothermal events that produced a complex assemblage of rocks and mineralization styles. REE deposits in China have attracted the attention of geologists in recent decades due to their high-grade, large-scale, and low Th content. The existing models for REE deposit formation include two important processes: REE-rich hydrothermal fluids exsolved from carbonatite-syenite complex then formed a REE deposit through precipitation of a combination of fluid cooling, mixing and phase separation.

The Miaoya REE prospect is hosted by a carbonatite–syenite complex in the Qinling Belt, China. Concentrations of REE, Ba, Sr, and other elements in this prospect are relatively high, similar to those at other large REE deposits such as those at Maoniuping and Dalucao. However, the REE minerals at the Miaoya prospect are rare than those deposits, which suggests that not all fertile carbonatites produce viable REE deposits. In the present study, XRD, LA-ICP-MS, EMPA, XRF, ICP-MS were employed to investigate trace element concentrations and the ratios of Sr, Nd, C, and O isotopes. Based on these results and the geological setting, the factors responsible for the low REE grades at the Miaoya prospect are subsequently discussed.

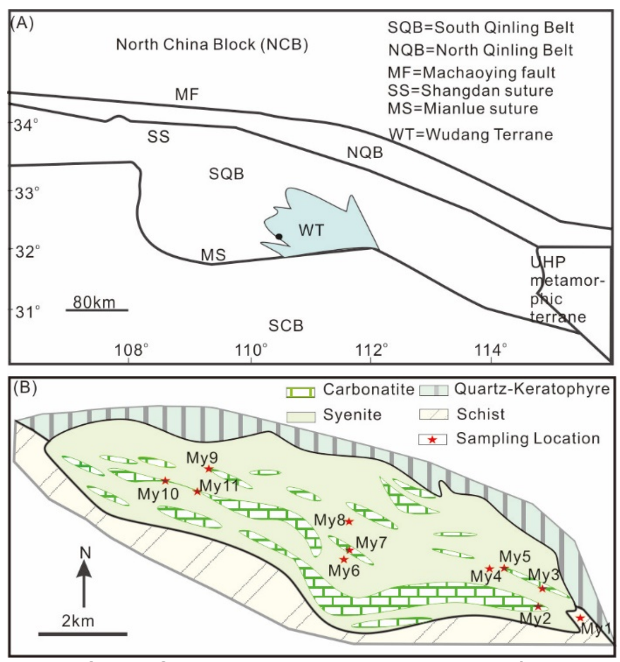

Figure.1 Sketch Geological Map showing the location of the Miaoya REE prospect (modified after Xu et al. 2010a).

2 Geological setting

The Miaoya REE prospect is located in the western area of the Wudan Terrane of the Qinling Belt. Forty-five shows have been discovered in a 12 square kilometer area with a total resource of 1.3 Mt TR_2O_3(Total weight in Metric tons of Rare Earth Element Oxides) and 0.9 Mt Nb_2O_5 (Ma et al. 1981). The prospect is hosted in a carbonatite-syenite complex (Xu et al. 2010a; 2010b) which intruded along the fault belt between the schist of the Lower-Silurian Meiziya group and the Proterozoic meta-quartz keratophyre of the lower Sinian Yaolinghe group of the Nahua formation. Carbonatite intruded the syenite as stocks and minor dikes. Li (2018) reported that a biotite K-Ar age yielded an age of 278 Ma for carbonatite. The U-Pb age of small oscillatory-zoned zircon from carbonatite was 147 ± 0.5, while the U-Pb age of large euhedral oscillatory-zoned zircon from carbonatite was 766 ±25Ma (Xu et al. 2012; 2015). Syenite predominantly consists of K-feldspar with minor albite, biotite, quartz, sericite, plagioclase, and calcite. Carbonatite consists of fine to medium grained calcite and minor K-feldspar, albite, augite, biotite, fluorapatite, columbite, bastnäsite, ilmenite, pyrochlore, quartz, monazite, aeschynite, ilmenorutile, rutile, and minor sulphides. The REE minerals, dominated by monazite and bastnäsite, fill fractures in calcite and feldspar.

3 Results

3.1 Chemical composition of syenite and carbonatite

A total of 11 carbonatite and syenite samples were analyzed. The results show that the carbonatites are characterized by: (1) low SiO_2, generally less than 20%; (2) low Al_2O_3 due to lacking of Al-silicates; (3) high CO_2 content, generally 25%-40%; (4) CaO+ MgO+ Fe_2O_3+ FeO ranging from 35% to 50%; and (5) compared to other igneous rocks, carbonatite contains higher TiO_2, MnO, BaO, SrO, and P_2O_5. The syenite has relatively higher SiO_2 (36.0%-60.6%), Al_2O_3 (11.8%-20.2%),Fe_2O_3(2.58%-4.35%),K2O(4.09%-8.40%) than carbonatite (SiO_2: 3.15%-13.5%; Al_2O_3:0.60%-5.77%; Fe_2O_3: 0.92%-1.28%; K_2O:0.17%-2.18%) while lower CaO (0.71%-16.8%) than carbonatite (36.3%-48.8%).

Typical samples of syenite and carbonatite ores are enriched in large-ion-lithophile elements. The light REE (La, Ce, Pr, Nd, Sm, and Eu) content of the samples (5800–74,000 ppm) is~46–~164 times those of the heavy REE (Gd, Tb, Dy, Ho, Er, Tm, Yb, Y, and Lu)

3.2 REE minerals in the Miaoya prospect

Both syenite and carbonatite samples have different mineral assemblages. Macroscopic and microscopic examination reveals the carbonatite contains higher amounts of calcite (58.5- 92.0 vol.%), mica (3.00-25.8 vol. %), apatite (1.1-17.3 vol.%), ankerite (2.0-13.9 vol.%), and minor plagioclase (0-0.9%), K-feldspar (0.5-1.0 vol.%), chlorite (0-3.0% vol.%), and quartz (0-5.0% vol.%), while the syenite samples are composed mainly of feldspar (16.0-25.9vol.%), mica (21.2-56.7vol.%) , quartz (9.5-20.8vol.%), calcite (0-27.0vol.%), ankerite (0-17.0vol.%), and apatite (0-4.4vol.%). The most obvious characteristics are that syenite contains relatively high amount of plagioclase, mica and quartz while carbonatite has more calcite and ankerite. Our XRD, SEM, BSE imaging, and EMPA data indicate that monazite, rather than bastnäsite, is the main primary REE mineral in the carbonatite at the Miaoya prospect, and monazite crystals are fine grained (10-100 μm), and rarely coarser-grained (<10 mm).

3.3 Minerals chemistry using LA ICP-MS

The apatite has high concentrations of Sr (5600-14600 ppm, ave.11000 ppm), Y (234-967 ppm, ave. 442 ppm); Th (4.3-312 ppm, ave. 65.9 ppm); U (0.05-30.3 ppm, ave. 6.4 ppm) and low concentrations of Rb (0.03-0.20 ppm, ave. 0.08 ppm), and HFSE (Zr:0.47-24.6 ppm, ave. 4.52 ppm; Hf: 0.01-0.18 ppm, ave. 0.07 ppm; Nb:0.35-5.67 ppm, ave. 1.37 ppm; Ta:0.00-0.10 ppm, ave.0.02 ppm)

Two types of calcite were identified at the Miaoya REE prospect based on total REE concentrations: calcite from schist and syenite (low total REE concentration), and calcite from carbonatite (high total REE concentration). The schist/syenite calcite also has high Rb (0.15 - 29.8 ppm) and lower HFSE than the carbonatite calcite.

In terms of the REE patterns of these individual minerals, the chondrite-normalized REE patterns for apatite exhibit negative slopes and lack an Eu anomaly. Calcite from carbonatite has a right-dip trend patterns with $(La)_N/(Lu)_N$ (0.24-322, ave. 57.1), while the calcite from schist and syenite has low concentration of all the trace elements, and has flat REE patterns. Columbite and ilmenite have an average REE up to 1000 ppm. The trace element concentrations in augite, biotite, plagioclase, and quartz are low, below 10 ppm, and they show a positive Eu anomaly.

3.4 Sr-Nd and C-O isotopes

Most samples have high Sr content, 3200 ppm to 5700 ppm in carbonatite, 2000 ppm to 2200 pp in mixed rocks and 4900 ppm in mixed carbonatite. The Sr in syenite (128 -11000 ppm) and schist (404 ppm) are relatively low. The initial $^{87}Sr/^{86}Sr$ (0.7038 to 0.7095) and $^{143}Nd/^{144}Nd$ (0.512269 to 0.512439) isotope ratios of different samples remain constant (Figure 1).

The carbonatite exhibits $\delta^{18}O$ values of 11.1 ‰ to 13.8‰ and $\delta^{13}C$ values of –5.4‰ to –3.1 ‰; these compositions fall outside of the field of the typical primary mantle-derived carbonatite on a $\delta^{18}O_{V\text{-}SMOW}$ vs. $\delta^{13}C_{V\text{-}PDB}$ diagram where the consistent $\delta^{13}C_{V\text{-}PDB}$ value and highly variable $\delta^{18}O_{V\text{-}SMOW}$.

4 Discussion

4.1 REE enrichment at the Miaoya prospect

Three lines of evidence suggest that the Miaoya complex formed by unmixing of silicate magma: the syenites and carbonatites are spatially co-located, carbonatite and syenite yield similar Sr–Nd isotopic ratios, and trace element concentrations in syenite and carbonatite produce similar patterns on spider diagrams and REE plots (Hou et al.2015).

At the Miaoya prospect, measured Sr–Nd isotopic ratios for REE-mineralized carbonatites and syenites are similar to Sr–Nd ratios for fresh carbonatites and syenites. The Sr–Nd isotope ratios define isotopic arrays that deviate from the mantle array in a similar way to the EACL (East African Carbonatite Line), which was derived directly from the mantle without the involvement of REE-rich sedimentary material (Hou et al. 2015). Strontium and neodymium isotope ratios can be used to classify carbonatites as fertile or barren. Barren carbonatites follow the evolution trend of HIMU and EMI, while fertile carbonatites such as those at Bayan Obo, Weishan, and Mianning–Dechang deviate from this trend, as mentioned by Hou et al. (2015).

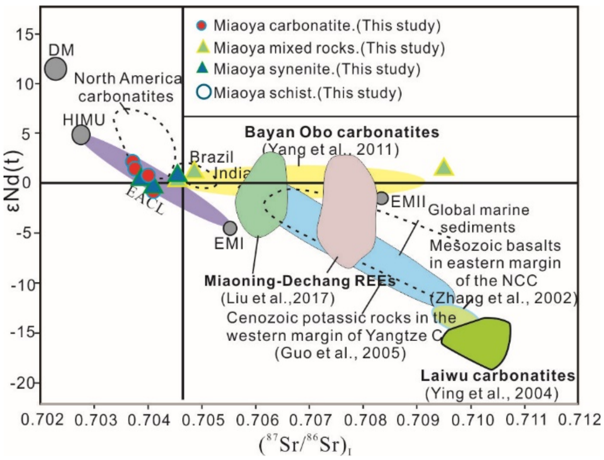

Figure 2. Whole rock Sr-Nd isotopic compositions of syenite and carbonates from the Miaoya REE prospect.

Carbonatites from the Miaoya prospect have high total REE concentrations (1300–4800 ppm) relative to the majority of the syenites (350–857 ppm REE), although one syenite sample contains 19,000 ppm REE. These concentrations, in combination with the genetic model inferred from the geological setting, suggest that carbonatites from Miaoya are typical fertile carbonatites, with potential for REE mineralization during magmatic–hydrothermal events. However, REE concentrations at Miaoya are lower than those at the Lizhuang, Maoniuping, and Dalucao deposits in the Mianning–Dechang REE belt (Hou et al.2015).

Only calcite and apatite hosted by carbonatite contain elevated concentrations of REE, with total REE concentrations up to 35,000 and 14,000 ppm, respectively (Fig.1). Columbite and ilmenite contain lower REE concentrations than apatite and cannot account for the REE mineralization. Monazite is one of the important REE minerals in carbonatite-related REE deposits (Chen et al. 2018) and is the most important primary REE mineral at the Miaoya prospect (Xu et al. 2010b; 2015; Ying et al. 2017). Both monazite and bastnäsite crystals are relatively small and rare.

Figure 2 shows the distinct isotopic arrays defined by barren and fertile carbonatite, dolomitic dikes with low REE concentrations have lower $^{87}Sr/^{86}Sr$ ratios than calcitic dikes at the Bayan Obo, suggesting that the Miaoya prospect involved lesser metasomatic refertilization and the addition of REEs and LILEs to the SCLM.DM.HIMU,EMI, and EMII are mantle end-members (i.e. depleted mantle (DM),High-μmantle (HIMU), Enriched mantle 1 （EM1）,and enriched mantle II (EMII); Hart etl al.,1992).

4.2 Evolution of ore-forming fluids

Low-temperature isotope exchange between carbonates, meteoric water, and magmatic fluids produces positive shifts in $\delta^{18}O$ values in carbonates during the evolution of hydrothermal fluids. Such changes in C–O isotopic compositions are observed between bulk primary carbonatite and hydrothermal calcite at the Miaoya prospect ($\delta^{18}O_{V\text{-}SMOW}$ = 11.1‰ to 13.8‰ and $\delta^{13}C_{V\text{-}PDB}$ = −4.9‰ to −3.5‰) . Carbon–oxygen isotopes, together with field observations of lithology, suggest that at least three possible fluid sources should be considered at the Miaoya prospect: meteoric water, magmatic water, and CO_2 derived from the decarbonation of carbonatite. In the absence of interaction with meteoric water, the syenite–carbonatite complex host rock and CO_2 produced by decarbonation would result in relatively high oxygen isotope ratios that are typical of hydrothermal fluids. At the Miaoya prospect, C–O isotope ratios suggest that meteoric water and CO_2 from decarbonation made minor contributions to the ore-forming fluids. Thus, magmatic water was the most likely primary contributor of fluid during mineralization.

4.3 Potential of carbonatite-syenite complexes for REE mineralization

Two REE-enrichment processes are necessary to form such deposits: production of fertile carbonatite and subsequent upgrade by magmatic–hydrothermal processes. Fertile carbonatites that host REE deposits commonly have high REE, Ba, and Sr contents, but fertility is not related to CaO:MgO or FeO:MgO ratios. Concentrations of REE, Ba, and Sr at Miaoya are lower than those at giant or large REE deposits elsewhere in the world, with data for Miaoya plotting in the barren field or near to the boundary between the barren and fertile fields in (REEs vs. CaO/MgO, FeO/MgO, Ba and Sr/Ba) diagrams (Fig.2). The low REE contents suggest that the carbonatite–syenite complex at the Miaoya does not have the potential to host large or giant REE deposits.

During the early stages of mineralization, local tectonic activity generally will produce fractures or fissures in carbonatite–syenite complexes, facilitating fluid cycling and modifying the fluid chemistry by water–rock interaction. Circulation of ore fluids in tectonic fractures drives alteration within the carbonatite and leads to high concentrations of REE, F^-, Cl^-, CO_2, $(SO_4)^{2-}$, and volatiles in the fluids. There is little evidence of tectonic activity within the Miaoya prospect, and petrography reveals a relatively intact inner structure in altered syenites and carbonatites. Microprobe and BSE imaging reveal that calcite grains show clear mineral boundaries and clear cleavages; these features are rare in the altered carbonatite complexes that host the Mianning–Dechang REE deposits, which would have hindered the cycling of hydrothermal fluids.

Sulfate and fluorite ions form stable complexes with the REE and could be important for REE transport and precipitation, respectively (Williams-Jones et al. 2012). REE-sulfate and -carbonate complexes are particularly important at high-temperature and mildly acidic to near-neutral pH conditions (Williams-Jones et al. 2012 ; Migdisov and Williams-Jones 2014). Large and giant REE deposits generally contain large amounts of fluorine- and sulfate-bearing minerals, such as fluorite, fluorapatite, barite, and celestite, as the main gangue minerals. The abundance of these minerals implies high fluoride and sulfate contents in the ore-forming fluids (Kynicky et al. 2012). However, fluorite and barite are rare at the Miaoya prospect, suggesting that fluorine and sulfate contents were low in the ore-forming fluids, with a consequent reduction in transport and precipitation of REE. We conclude that a low concentration of suitable ligands for REE is another factor that inhibited REE mineralization at the Miaoya prospect.

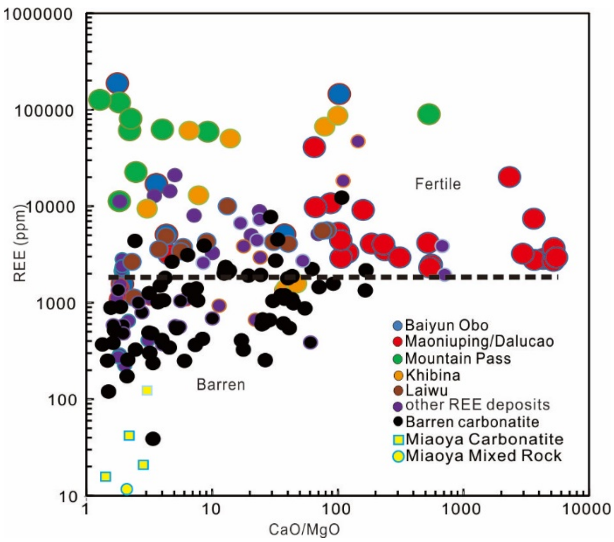

Figure 3. (A) REEs Vs.CaO/MgO diagrams of main global examples of carbonatites.

5 Conclusions

Two lines of the evidence suggest that REE at the Miaoya prospect were derived from the carbonatite–syenite complex itself: (1) the Sr–Nd isotope values of altered syenite and carbonatite are similar to those of fresh carbonatite and syenite; and (2) trace-element contents of apatite and calcite in mineralized samples are similar to those in unaltered samples, indicating that apatite and calcite in the carbonatites were the original source of REE for the deposit.

Three factors contributed to the low grade of ores at the Miaoya prospect: (1) REE concentrations in the carbonatite–syenite complex are lower relative to those in carbonatites at large and giant deposits; (2) there was little tectonic activity subsequent to intrusion, which restricted the extent of hydrothermal activity; and (3) low contents of fluorite, barite, calcite, and celestite in the prospective ores suggest that F^-, $(SO_4)^{2-}$, CO_2, and other volatile components that are necessary to transport and facilitate the precipitation of REE were not present in sufficient concentrations at the Miaoya prospect.

Acknowledgements

Acknowledgments: This research was funded by [National Key R&D Program of China] grant number [2017YFC0601503] and [National Natural Foundation of Science of China] grant number [41672082], [41472301] and [41772044]. The authors sincerely thank Qisheng Hu and Qianyu Zhao from Eighth Geological Brigade of Hubei Province for theirs great assistance in field survey.

References

Chen W, Lu J, Jiang SY, Ying YC, Liu YS (2018) Radiogenic Pb reservoir contributes to the rare earth element (REE) enrichment in South Qinling carbonatites Chemical Geology

Hou Z, Liu Y, Tian S, Yang Z, Xie Y (2015) Formation of carbonatite-related giant rare-earth-element deposits by the recycling of marine sediments Scientific Reports 5:10231

Kynicky J, Smith MP, Xu C (2012) Diversity of Rare Earth Deposits: The Key Example of China Elements 8:361-367

Li XC, Zhou MF (2018) The Nature and Origin of Hydrothermal REE Mineralization in the Sin Quyen Deposit, Northwestern Vietnam Economic Geology 113:645-673

Ma YX, Zhu HM, Gu TH (1981) Report for Detailed investigation of Miaoya Nb and REE deposit area in Zhushan County, Hubei Province (unpublished).

Migdisov AA, Williams-Jones AE (2014) Hydrothermal transport and deposition of the rare earth elements by fluorine-bearing aqueous liquids Mineralium Deposita 49:987-997

Williams-Jones AE, Migdisov AA, Samson IM (2012) Hydrothermal mobilisation of the Rare Earth Elements – a Tale of "Ceria" and "Yttria" Elements:355-360

Xu C, Kynicky J, Chakhmouradian AR, Campbell IH, Allen CM (2010a) Trace-element modeling of the magmatic evolution of rare-earth-rich carbonatite from the Miaoya deposit, Central China Lithos 118:145-155

Xu C, Wang L, Song W, Wu M (2010b) Carbonatites in China: A review for genesis and mineralization Geoscience Frontiers 1:105-114

Xu C, Taylor RN, Li W, Kynicky J, Chakhmouradian AR, Song W (2012) Comparison of fluorite geochemistry from REE deposits in the Panxi region and Bayan Obo, China Journal of Asian Earth Sciences 57:76-89

Xu C, Kynicky J, Chakhmouradian AR, Li X, Song W (2015) A case example of the importance of multi-analytical approach in deciphering carbonatite petrogenesis in South Qinling orogen: Miaoya rare-metal deposit, central China Lithos 227:107-121

Ying Y, Chen W, Lu J, Jiang S-Y, Yang Y (2017) In situ U–Th–Pb ages of the Miaoya carbonatite complex in the South Qinling orogenic belt, central China Lithos 290-291:159-171